



Collaborative multidepot electric vehicle routing problem with time windows and shared charging stations

Yong Wang^{a,*}, Jingxin Zhou^a, Yaoyao Sun^b, Jianxin Fan^c, Zheng Wang^d, Haizhong Wang^e

^a School of Economics and Management, Chongqing Jiaotong University, Chongqing 400074, China

^b School of Economics and Management, Nanjing University of Aeronautics and Astronautics, Nanjing 211106, China

^c School of River and Ocean Engineering, Chongqing Jiaotong University, Chongqing 400074, China

^d School of Maritime Economics and Management, Dalian Maritime University, Dalian 116026, China

^e School of Civil and Construction Engineering, Oregon State University, Corvallis, OR 97330, USA



ARTICLE INFO

Keywords:

Collaborative mechanism
Multidepot electric vehicle routing problem with time windows
Shared charging stations
Bi-objective nonlinear programming model
Improved multi-objective genetic algorithm with tabu search

ABSTRACT

Logistics distribution using electric vehicles (EVs) is gradually becoming popular in urban logistics networks with the promise of carbon peak and carbon neutrality. A collaborative mechanism among multiple depots can effectively increase the efficiency and sustainability of a logistics network. Sharing charging stations (CSs) is presented as a critical strategy to improve the efficiency of logistics networks and facilitate collaboration further. Solving a collaborative multidepot EV routing problem with time windows and shared charging stations (CMEVRPTW-SCS) involves centralized transportation services among multiple depots, coordinated delivery services among multiple depots and the charging needs of EVs. A bi-objective nonlinear programming model for CMEVRPTW-SCS is formulated to minimize the total operating cost and number of EVs, wherein the operating cost contains transportation costs among depots and vehicle routing costs in each depot. Gaussian mixture clustering algorithm is developed to cluster customers and assign them to depots probabilistically to reduce the computational complexity, and an improved multi-objective genetic algorithm with tabu search (IMOGA-TS) is designed to optimize the EV routes and charging locations in CMEVRPTW-SCS. With the combination of local and global searches and the improvement of solutions at each iteration by TS, the proposed hybrid algorithm can significantly accelerate the efficient exploration of optimal solutions. The comparative results of the IMOGA-TS with multi-objective genetic algorithm, non-dominated sorting genetic algorithm-II and multi-objective harmony search algorithm show the superiority of the proposed algorithm in solving CMEVRPTW-SCS. Then, a Shapley value model based on game theoretical methods is proposed to find the best profit allocation scheme. A real-world case study of CMEVRPTW-SCS in Chongqing City, China is conducted, and three scenarios of various collaborative alliances and 11 schemes with and without shared CSs are further discussed. The experimental results show that the proposed methods are of practical significance in reducing operating costs, improving transportation efficiency, and achieving sustainable operation in EV-based logistics distribution networks.

1. Introduction

The rapid development of urban logistics and transportation brings many negative social impacts, such as the increase in traffic congestion, the emission of harmful gases, and the exacerbation of global warming (Keskin, Çatay, & Laporte, 2021; Yang, Ning, Tong, & Shang, 2021). Governments of countries begin to introduce relevant policies and

regulations to promote environment-friendly electric vehicles (EVs) to replace traditional fossil fuel vehicles, and encourage the construction of sustainable logistics distribution networks (Keskin, Laporte, & Çatay, 2019; Asghari and Al-e-hashem, 2021). However, given the constraints of battery capacity, EVs need to be charged frequently at charging stations (CSs) (Erdelic et al., 2019). The lack and privatization of CSs have put increasing pressure on logistics enterprises to build efficient and

Peer review under responsibility of Submissions with the production note 'Please add the Reproducibility Badge for this item' the Badge and the following footnote to be added: The code (and data) in this article has been certified as Reproducible by the CodeOcean: <https://codeocean.com>. More information on the Reproducibility Badge Initiative is available at <https://www.elsevier.com/physicalsciencesandengineering/computerscience/journals..>

* Corresponding author.

E-mail addresses: yongwx@cqjtu.edu.cn (Y. Wang), jxfanw@cqjtu.edu.cn (J. Fan), drwz@dlut.edu.cn (Z. Wang), Haizhong.Wang@oregonstate.edu (H. Wang).

low-cost logistics networks (Koç, Jabali, Mendoza, & Laporte, 2019). In addition, the short-range and limited loading capacity of EVs and the continuing growth of road freight transportation volume inevitably lead to unreasonable EV scheduling and facility coordination in logistics networks, which consist of multiple depots and large number of customers (Lu, Chen, Hao, & He, 2020). In particular, customer service can be shared among multiple depots, in other words, depots can cooperate with one another and share customer service. The linkages are determined according to which depot serves which customers are reallocated on the basis of the optimization results to minimize the total cost and improve distribution efficiency. Therefore, the optimization of the EV-based distribution network by designing reasonable collaborative mechanisms to coordinate various facilities and implementing customer service and CS sharing strategies to reduce transportation costs is particularly important for logistics operators.

The EV-based distribution network consists of multiple depots, several CSs, a fleet of EVs, and a large number of customers. In this distribution network, multidepot EV routing optimization and the application of collaborative mechanism among logistics facilities are beneficial to reduce operating costs and promote transportation efficiency for logistics enterprises (Karakatić, 2021; Wang, Zhang, et al., 2021). In a collaborative logistics network, customer service sharing can be realized via the construction of collaborative alliances among multiple depots to avoid irrational staggered transportation and reduce operating costs (Cleophas, Cottrill, Ehmke, & Tierney, 2019; Wang, Yuan, et al., 2020). Currently, CSs, the essential facilities in an EV distribution network are usually privately owned by enterprises, that is, an EV can only be charged at the CSs of the same company (Montoya, Guéret, Mendoza, & Villegas, 2017; Pardo-Bosch, Pujadas, Morton, & Cervera, 2021). Moreover, the imbalance between the charging demands of EVs and the layout of CSs results in the low utilization of CSs. For example, the ratio of EVs to CSs in China was about 3:1, while the average utilization rate of CSs was less than 10 % in 2021 (CEVCIPA, 2021). Typically, the charging demands of EVs occur in urban areas, resulting in the short supply of CSs in urban centers (CCTV.com, 2021). Sharing CSs among multiple depots to facilitate collaboration is a useful strategy to deal with the current unreasonable use of CSs (Koç et al., 2019). Centralized transportation services among multiple depots and vehicle routing in each depot can be considered in the collaborative logistics network, and the transportation requirements need be merged or transshipped, and then additional profits will be generated with a transformative process from a non-optimal network to an optimal one (Wang et al., 2017). In addition, appropriate profit allocation methods should be designed in the construction of collaborative alliances to maintain the stability and sustainability of collaboration (Wang, Peng, and Xu, 2021).

The collaborative multidepot EV routing problem with time windows and shared charging stations (CMEVRPTW-SCS) is proposed and solved in this study, in which the delivery tasks and charging requirements of EVs can be coordinated among multiple depots via a collaborative optimization network framework. In the collaborative framework, customer service sharing is adopted to reduce transportation costs, and CS sharing is incorporated to facilitate the rational use of CSs and improve the utilization of EVs. Integrating collaboration based on customer service and CS sharing among multiple depots is beneficial to improve the efficiency of the EV distribution network (Muñoz-Villamizar, Montoya-Torres, & Faulin, 2017; Koç et al., 2019). The proposed CMEVRPTW-SCS is formulated as a bi-objective nonlinear programming model to minimize the total operating cost and the number of EVs simultaneously. A hybrid algorithm consisting of the Gaussian mixture clustering algorithm (GMCA) and the improved multi-objective genetic algorithm with tabu search (IMOGA-TS) algorithm is developed to solve the proposed problem. The GMCA is employed to assign customers to appropriate depots for reducing the complexity of logistics network optimization, and the IMOGA-TS is designed to search the optimal routes and obtain the best charging decisions simultaneously. Then, a

profit allocation strategy based on cooperative game theory is introduced to allocate profits among the collaborative participants and promote the stability of collaborative alliances.

The remaining sections of this study are organized as follows. Section 2 summarizes the literature on existing problems and solution methods related to the CMEVRPTW-SCS. Section 3 proposes a simplified example of CMEVRPTW-SCS. Next, Section 4 illustrates the related definitions and model formulation. Then, Section 5 describes a hybrid algorithm consisting of GMCA and IMOGA-TS, and it introduces a Shapley value model to allocate profits among multiple participants. Afterward, Section 6 presents a real-world case study to verify the applicability and effectiveness of the proposed model and algorithms. Lastly, Section 7 summarizes this study and provides future research directions.

2. Literature review

With the increasing awareness on environmental protection, the optimization study on the EV routing problem (EVRP) has attracted the attention of several researchers and logistics managers (Schiffer & Walther, 2017; Asghari and Al-e-hashem, 2021; Zang, Wang, & Qi, 2022). Variants such as time windows and multidepot are commonly added to the standard EVRP, thus resulting in the evolution of two extensions, namely, EVRP with time windows (EVRPTW) and multidepot EVRPTW (MDEVRPTW) (Hiermann, Puchinger, Ropke, & Hartl, 2016; Keskin & Çatay, 2018; Kucukoglu, Dewil, & Catrysse, 2021). Given the economic and environmental impacts, collaborative mechanism and resource sharing have been increasingly studied by researchers as promising strategies (Cleophas et al., 2019; Zon & Desaulniers, 2021). Additionally, relevant methodologies for EVRP are also diversified in the existing literature (Konstantakopoulos, Gayialis, & Kechagias, 2020; Moghdani, Salimifard, Demir, & Benyettou, 2021; Cai, Wang, Luo, & Liang, 2022). The CMEVRPTW-SCS in this study not only combines charging decisions and travel routing schemes of EVs, but also introduces collaboration and CS sharing strategies among multiple depots. This section will summarize the relevant literature of CMEVRPTW-SCS from three aspects as follows: problems, strategies, and solution methods.

2.1. Evrptw

The growing concern about climate change and greenhouse gas emissions has strongly motivated research on green logistics, and EVRP is one of the main directions to address these concerns (Schiffer & Walther, 2017; Keskin & Çatay, 2018; Granada-Echeverri, Cubides, & Bustamante, 2020). Generally, EVs need to be charged at CSs due to their limited driving ranges and battery capacities (Keskin et al., 2019). Lin, Zhou, and Wolfson (2016) studied the vehicle loading effect on battery consumption and presented an EVRP model to minimize the cost of travel time, energy, and number of EVs in the process of finding optimal routes. Zhang, Gajpal, Appadoo, and Abdulkader (2018) developed a comprehensive calculation model of energy consumption in EVRP to demonstrate the superiority of objective function based on minimum energy consumption. Shao, Guan, and Bi (2018) introduced a nonlinear energy consumption function into the EVRP model to discuss the influence of vehicle speed and load capacity on routing optimization. EVRPTW was further studied by several researchers due to the significance of time windows in the real-world (Keskin & Çatay, 2018; Kucukoglu et al., 2021). Keskin and Çatay (2018) designed an EVRPTW with three charging types, namely, ordinary, fast, and overcharge modes, and assumed that the charging time is linear and related to the charging mode. Cortés-Murcia, Prodhon, and Afsar (2019) considered serving customers by walking during the charging period to reduce the charging time in EVRPTW. Granada-Echeverri et al. (2020) formulated a mixed-integer linear programming model to reduce the return of empty vehicles and improve the transportation efficiency of EVs in EVRPTW. Chen, Li, Zhang, Wahab, and Jiang (2021) developed an integer programming

model to select the location of battery swap stations and optimize EV routes under the constraints of driving range, load capacity, and time windows. Raeesi and Zografos (2022) introduced a route planning model to achieve cost and emission savings and coordinated the routing of EVs with intra-route recharging and en-route battery swapping in solving a variant of EVRPTW.

2.2. Mdevrptw

Recently, a growing number of studies have been dedicated to MDEVRPTW as concerns have been raised about the related technology and development of EVs for enterprises (Kucukoglu et al., 2021). Wen, Linde, Ropke, Mirchandani, and Larsen (2016) addressed an EV scheduling problem, which allows each electric bus to start and end at a specific depot and time, and to be fully or partially charged at specified CSs. Furthermore, Li, Soleimani, and Zohal (2019) developed a multi-depot green vehicle routing problem to maximize revenue and minimize costs, time, and emission for efficiently saving the potential cost and improving the service. In addition, Erdem and Koç (2019) proposed an EVRP in the area of home health care, and analyzed the influence of various factors, such as preference, skill matching, synchronization, heterogeneous EV fleets, and charging strategies, on transport distance. Almouhanna et al. (2020) studied the location routing problem with different depot capacities and allowed all EVs to be shared among the depots. Karakatić (2021) designed a MDEVRPTW model to minimize driving times, number of stops at CSs, and charging time. Moreover, Ghobadi, Tavakkoli-Moghaddam, Fallah, and Kazemipoor (2021) presented a MDEVRPTW to minimize the travel distance cost and the penalty cost of violating time windows from the perspective of economy and customer satisfaction. In another study, Wu, Lin, Liu, and Jin (2022) developed a bi-objective optimization model in the multidepot EV scheduling problem to solve the high operating cost and the unbalanced charging demand.

2.3. Collaboration and resource sharing for MDEVRPTW-SCS

With the intensification of logistics industry competition and the enhancement of human environmental awareness, collaboration has attached researchers' attention as a promising strategy for improving the efficiency of modern logistics networks (Mancini, Gansterer, & Hartl, 2021; Aloui, Hamani, & Delahoche, 2021; Wang, Wang, et al., 2022). Resource sharing, as a strategy to achieve collaboration, such as CS sharing and customer service sharing, can effectively reduce operating costs and improve the EV transportation efficiency (Muñoz-Villamizar et al., 2017; Koç et al., 2019). Muñoz-Villamizar et al. (2017) proposed a collaborative strategy based on customer service sharing to reduce the total cost and improve efficiency in an urban logistics system. Furthermore, Clephas et al. (2019) analyzed different collaborative approaches including vertical and horizontal from the view of operation research and discussed various collaborative forms, such as shared customer service, shared vehicles, multiple facilities collaboration. Meanwhile, Koç et al. (2019) developed a CS sharing strategy to build CSs jointly by multiple companies and required enterprises to share distribution centers and customer service information to obtain more benefits. Li, Lim, Tan, Lee, and Tseng (2020) investigated the effect of power distribution sharing and formulated a routing optimization model for EV routing problem based on power-sharing. Li, Lim, and Wang (2022) integrated blockchain technology into urban logistics distribution system to realize horizontal cooperation and designed an open vehicle routing model to achieve the lowest total cost.

Collaboration and resource sharing inevitably involve the profit distribution of participants, and game theory is often used to study the distribution of profits among participants (Wang et al., 2017; Santos, Martins, Amorim, & Almada-Lobo, 2021). Wang, Yu, and Tang (2018) proposed an exact calculation method to compute the distribution of actual compensation and profit on the basis of cooperative game

theories for the green pickup and delivery problem. Furthermore, Vaziri, Etebari, and Vahdani (2019) proposed a new VRP with fair carrier collaboration and built a mixed-integer programming model to maximize total cost savings and achieve fair profit distribution among carriers. In another study, Jouida, Guajardo, Klibi, and Krichen (2021) modeled three sharing mechanisms including egalitarian distribution, proportional distribution, and Shapley value to test the performance of collaboration in reducing costs and increasing revenues. Zon and Desaulniers (2021) developed a collaborative game model to determine the allocation scheme of the additional profits from the integration of customer demands, delivery routes, and new customer services.

2.4. Relevant solution methods for CMEVRPTW-SCS

Solution methods proposed by researchers for solving VRP and its variants mainly consist of exact and heuristic approaches (Konstantopoulos et al., 2020). As EVRP is an NP-hard problem, most scholars prefer to use heuristic methods as solution methodologies (Roberti & Wen, 2016; Moghdani et al., 2021). For instance, Goeke and Schneider (2015) developed an adaptive large neighborhood search (ALNS) algorithm to solve EVRPTW with mixed fleets and designed four local search (LS) operators to expand solution space. Meanwhile, Keskin and Çatay (2016) designed several new mechanisms specifically for EVRPTW to remove or insert CSs according to their previous performances dynamically and adaptively. Zhang, Chen, and Zhang (2019) proposed a hybrid algorithm that incorporated Pareto optimality into particle swarm optimization (PSO) and variable neighborhood search (VNS) to achieve a scheme with minimal cost in an EV location-routing problem. Rezgui, Chaouachi Siala, Aggoune-Mtalaa, and Bouziri (2019) presented a VNS to find the optimal routing of the last-mile delivery by exploring increasingly neighborhoods of candidate solutions and changing the solution only if it improves. Bac and Erdem (2021) developed a series of neighborhood operators for VNS and variable neighborhood descent (VND) heuristics to optimize the recharging time, number of EVs and used CSs. Nolz, Absi, Feillet, and Seragiotti (2022) proposed an ALNS with constraint and quadratic programming to use limited charging resources efficiently and optimize the vehicle fixed cost in solving the consistent EVRP with backhauls and charging management.

As one typical algorithm of metaheuristic methodologies, MOGA is widely applied to solve multi-objective optimization problems (Xu, Elomri, Pokharel, & Mutlu, 2019; Ghannadpour and Zandiye, 2020). Additionally, TS, as an effective strategy to improve algorithm performance and expand search space, is often embedded into other algorithms (Verma, 2018; Gmira, Gendreau, Lodi, & Potvin, 2021). Schneider, Stenger, and Goeke (2014) proposed a hybrid heuristic algorithm combining VNS with TS to solve EVRPTW and designed a new, problem-specific operator to insert or remove CSs. Meanwhile, Yang and Sun (2015) designed a two-phase TS-modified Clarke and Wright savings heuristic to determine the location strategy of BSSs and the routing plan of a fleet of EVs simultaneously under battery driving range limitation. Moreover, Soto, Sevaux, Rossi, and Reinholz (2017) developed a hybrid algorithm combining multiple neighborhood search and TS strategies to address a multidepot open vehicle routing problem. Pierre and Zakaria (2017) developed a MOGA with the stochastic partially optimized cyclic shift crossover to improve algorithm performance in solving VRPTW. Furthermore, Goeke (2019) developed a granular TS with a charging policy to ensure the feasibility of energy consumption and satisfy the time windows of customers in the pickup and delivery problem with EVs. Hiermann, Hartl, Puchinger, and Vidal (2019) designed a sophisticated metaheuristic combining a GA with LS and LNS to solve EVRP and introduced CS insertion strategies including labeling techniques and greedy evaluation in a fixed trip. In addition, Ghannadpour & Zandiye (2020) designed a MOGA incorporating several heuristic algorithms into crossover, mutation, and hill-climbing operators to solve VRPTW. Sadati, Çatay, and Aksen, (2021) presented a

Table 1

Relevant literature overview for CMEVRPTW-SCS.

References	Variants		Electric fleet transportation			Strategy		
	Multidepot	Multi-echelon	Time windows	Homogeneous	Heterogeneous	Collaboration	CS sharing	Customer service sharing
Schneider et al. (2014)			✓	✓				
Goeke and Schneider (2015)			✓		✓			
Desaulniers, Errico, Irnich, and Schneider (2016)			✓	✓				
Hiermann et al. (2016)			✓		✓			
(Keskin and Çatay, 2016)			✓	✓				
Muñoz-Villamizar et al. (2017)	✓		✓	✓		✓	✓	✓
Schiffer and Walther (2017)			✓	✓				
Shao et al. (2018)			✓	✓				
Verma (2018)			✓	✓				
Cortés-Murcia et al. (2019)			✓		✓			
Erdem and Koç (2019)	✓		✓		✓			
Goeke (2019)			✓					
Hiermann et al. (2019)	✓	✓			✓		✓	
Koç et al. (2019)				✓				
Li et al. (2019)		✓		✓				✓
Zhang et al. (2019)				✓				
Almouhanna et al. (2020)			✓		✓			
Li et al. (2020)			✓	✓		✓		
Wang, Yuan, et al. (2020)	✓	✓	✓	✓		✓	✓	
Karakatić (2021)				✓				
Bac and Erdem (2021)				✓				
Cai et al. (2022)				✓				
Raeesi and Zografos (2022)				✓				
This work	✓	✓	✓			✓	✓	✓

variable Tabu neighborhood search algorithm to escape from local optima and obtained a high-quality feasible solution for solving multidepot vehicle routing problem (MDVRP). Cai et al. (2022) developed a hybrid ALNS and TS algorithm to optimize vehicle routes with the highest total profit in solving the EV relocation problem.

Table 1 summarizes relevant studies for CMEVRPTW-SCS. The column headings stand for multidepot, multi-echelon, time windows, electric fleet transport, and strategy. The abbreviations in the study are specified as follows.

EVRP: EV routing problem

MEVRPTW-SCS: Multidepot EV routing problem with time windows and shared charging stations

MDEVRPTW: Multidepot EV routing problem with time windows
CMEVRPTW-SCS: Collaborative multidepot EV routing problem with time windows and shared charging stations

GMCA: Gaussian mixture clustering algorithm
IMOGA-TS: Improved multi-objective genetic algorithm with tabu search

The limitations of relevant literature for MEVRPTW-SCS optimization can be summarized as follows: (1) Collaborative mechanisms have not been sufficiently studied in MDEVRPTW, that is, the sharing of logistics facilities and customers' service among multiple depots are rarely investigated in EVRP. (2) The application of CS sharing strategy in the multidepot EV delivery network optimization has not been fully studied,

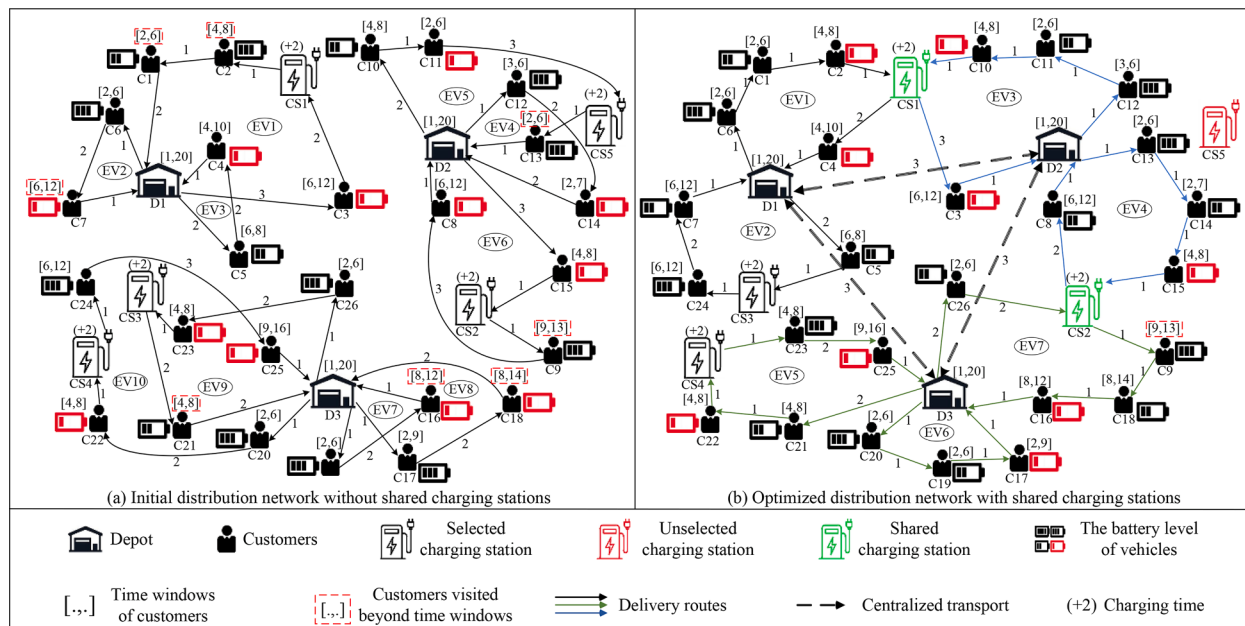


Fig. 1. Illustration of CMEVRPTW-SCS optimization.

Table 2

Service relationship characteristics among depots.

Depot	Initial		Optimized	
	Customers	CSs	Customers	CSs
D1	C1-C7	CS1	C1, C2, C4-C7, C24	CS1-CS5
D2	C8-C15	CS2, CS5	C3, C8, C10-C15	CS1-CS5
D3	C16-C26	CS3, CS4	C9, C16-C23, C25, C26	CS1-CS5

which means the effects of the CS sharing on the EV utilization and the cost reduction of logistics networks have rarely been explored. (3) A valid mathematical model formulation for the collaborative mechanism and the CS sharing strategy in the CMEVRPTW-SCS optimization is currently lacking. (4) Existing evolutionary algorithms and heuristic approaches are difficult to apply to solve CMEVRPTW-SCS directly.

Compared with previous studies, this study has the following contributions. (1) A collaborative mechanism is proposed in the MDEVRPTW to facilitate collaborative customer service and obtain effective EV route planning. (2) A CS sharing strategy is employed in the proposed CMEVRPTW-SCS to optimize charging decisions and EV scheduling. (3) A bi-objective nonlinear mathematical programming model integrating customer service sharing, CS sharing, and centralized transportation demands is established to minimize the total operating cost and number of EVs in CMEVRPTW-SCS. (4) A two-stage solution method consisting of GMCA and IMOOGA-TS is proposed to solve the bi-objective nonlinear optimization model and obtain the optimal solution efficiently.

3. Problem statement

CMEVRPTW-SCS aims to optimize a logistics network by establishing a collaborative mechanism among multiple depots, and sharing CSs and customer service to reduce the total operating cost and the environmental impact of logistics operations. The phenomenon of long-distance transportation often occurs in logistics networks, and the customer service sharing leads to the emergence of the transshipment of customer demands among multiple depots. Thus, centralized transportation and collaboration are commonly used to improve the mobility and organization of the logistics system (Muñoz-Villamizar et al., 2017; Wang, Zhang, et al., 2021). In CMEVRPTW-SCS, centralized transportation between multiple depots is performed by electric trucks (ETs), and customers are served within the specified time windows by their depots owning a fleet of EVs. To guarantee that EVs have enough energy when serving customers, EVs must be charged at their depots or CSs during the traveling process. In addition, CS sharing, customer service sharing, and centralized transportation for customers will help logistics companies utilize transportation resources effectively and reduce distribution trips in the CMEVRPTW-SCS. Collaborative alliances need to be established to ensure the operation of the collaboration mechanism, thereby achieving additional benefits by saving resource and reducing delivery distances. Meanwhile, allocating additional profits to alliance members by exploring appropriate profit allocation methods should be encouraged to maintain long-term and stable cooperation among multiple depots. Fig. 1 illustrates the CMEVRPTW-SCS optimization with a distribution network consisting of three depots (i.e., D1, D2, D3), five CSs (i.e., CS1, CS2, CS3, CS4, CS5), and 26 customers (i.e., C1-C26), and the numbers on delivery routes indicate the travel time of EVs. The customers served by three depots and their available CSs in the initial and optimized EV

distribution networks are listed in the Table 2.

In Fig. 1(a), the unreasonable distribution of customer service caused by the independent operation of depots leads to a large amount of long-distance and crisscross transportation routes, which further induces the violations of customers' time windows and the waste of electricity consumption. Moreover, when multiple depots do not cooperate with one another, most EVs have to be charged only at their corresponding depots or the depots' possessed CSs. Thus, inappropriate charging times and low utilization rates of a large number of EVs occur, thus leading to high charging costs and delivery costs. In Fig. 1(b), three CSs are shared among three depots to achieve a reduction in the number of used CSs, and the violation of customers' time windows is notably alleviated. In the optimized collaborative logistics network, the number of EVs required for distribution services and the electricity consumption of EVs are greatly decreased, and the logistics network is more orderly compared with the initial logistics network, due to the elimination of a great deal of unreasonable transportation. Furthermore, the CSs are shared, thus reducing the number of CSs used in the logistics network, enabling a smaller number of CSs to serve a larger number of customers, and then the remaining CSs can be shared and used by other depots or customer services at other times. Therefore, the establishment of a reasonable collaborative mechanism among multiple depots and the CS sharing strategy are effective for improving the resource utilization of both EVs and CSs, thus achieving a great reduction on the total operating cost. This is also conducive to propelling the sustainable development of an intelligent logistics system and the construction of a resource-friendly society.

We assume that the electricity consumption of EVs is only related to unit time, 10 kWh per unit time for electricity consumption (EC), \$2 per kWh for electricity prices, \$50 per EV for rental cost, \$10 per time unit for penalty cost (earliness and delay penalties), \$10 per time unit for charging cost, and \$30 per time unit for centralized transport cost. A comparison of rental cost (RC), electric delivery cost (EDC), penalty cost (PC), charging cost (CC), centralized transport cost (CTC), total operating cost (TOC), electricity consumption (EC), number of EVs, number of ETs, number of used CSs, and number of shared CSs before and after CMEVRPTW-SCS optimization is shown in Table 3.

In Table 3, all the operating costs, including rental cost, electric delivery cost, penalty cost, and charging cost, have been notably reduced. For example, the penalty cost is significantly decreased by 96 %, which denotes that the violations of customers' time windows have been greatly decreased. In addition, the electricity consumption is decreased from 650 to 490 kWh, and the electric delivery cost is decreased from \$2350 to \$1870, thus achieving a 20.4 % reduction in electricity consumption. Furthermore, the number of required EVs is significantly reduced from ten to seven, and the number of selected CSs is decreased by one as a result of the EV routing optimization. Therefore, the optimization of CMEVRPTW-SCS can reduce the total operating cost and raise the resource utilization efficiency of the logistics networks.

4. Related definitions and model formulation

4.1. Assumptions and definitions

The CMEVRPTW-SCS is formulated as a bi-objective nonlinear programming model to minimize the cost and number of EVs under the time windows and electricity capacity constraints. In this section, some relevant notations and variables adopted in the CMEVRPTW-SCS model

Table 3

Comparison in initial and optimized networks of CMEVRPTW-SCS.

Case	RC (\$)	EDC (\$)	PC (\$)	CC (\$)	CTC (\$)	TOC (\$)	EC (kWh)	Number of EVs	Number of ETs	Number of selected CSs	Number of shared CSs
Initial	500	1300	250	300	0	2350	650	10	0	5	0
Optimized	350	980	10	260	270	1870	490	7	1	4	2

Table 4

Notations and descriptions used in the CMEVRPTW-SCS model.

Set	Description
D	Set of depots, $D = \{1, 2, 3, \dots, d\}$, $d \in D$
C	Set of customers, $C = \{1, 2, 3, \dots, c\}$, $c \in C$
R	Set of charging stations, $R = \{1, 2, 3, \dots, r\}$, $r \in R$
V	Set of EVs, $V = \{1, 2, 3, \dots, v\}$, $v \in V$
TR	Set of ETs, $TR = \{1, 2, 3, \dots, t\}$, $t \in TR$
I	Set of all nodes, $I = D \cup C \cup R$
ε_v	Set of customers served by EV v , $v \in V$
Parameter	
δ_v	Arc specific coefficient of EV v , $v \in V$
ℓ_t	Arc specific coefficient of EV t , $t \in TR$
β_v	Vehicle specific coefficient of EV v , $v \in V$
τ_t	Vehicle specific coefficient of ET t , $t \in TR$
FV_v	Rental cost of EV v , $v \in V$
FT_t	Rental cost of ET t , $t \in TR$
F_d	Fixed cost of depot d , $d \in D$
μ_d	Variable cost coefficient of depot d , $d \in D$
f_e	Electricity price, (unit: \$)
f_{ch}	Charging cost of electricity per unit time, (unit: \$/h)
wv_v	Weight of EV v , $v \in V$, (unit: kg)
wt_t	Weight of ET t , $t \in TR$, (unit: kg)
a_v	Acceleration of EV v , $v \in V$, (unit: m/s ²)
g	Gravitational constant, (unit: m/s ²)
θ	Road inclination angle
λ_v	Rolling friction coefficient of EV v , $v \in V$
σ	Air drag coefficient
A_v	Frontal area of EV v , $v \in V$ (unit: m ²)
ρ	Air density, (unit: kg/m ³)
ζ_v	Drive train efficiency of EV v , $v \in V$
SV_v	Speed of EV v , $v \in V$, (unit: m/s)
ST_t	Speed of ET t , $t \in TR$, (unit: m/s)
δ_v	Charging rate of EV v , $v \in V$, (unit: kWh/h)
PE_d	Penalty cost per unit of time of earliness
PL_d	Penalty cost per unit of time of delay
M	Extremely large number
E_v	Battery capacity of EV v , $v \in V$, (unit: kWh)
SOC_{min}	Minimum state of charge of EV v , $v \in V$
l_{max}	Maximum travel distance of EV v , $v \in V$ (unit: km)
Q_v	Load capacity of EV v , $v \in V$, (unit: kg)
U_t	Load capacity of ET t , $t \in TR$, (unit: kg)
Variable	
θ_{ijv}	Description
θ_{ijv}	Second-by-second power required by EV v to overcome the resistance from node i to j , $v \in V$, $i, j \in I$, (unit: kw)
φ_{ijv}	Energy consumption of EV v from node i to j , $v \in V$, $i, j \in I$, (unit: kWh)
ψ_{ijv}	Energy consumption of ET t from depot d to d' , $t \in TR$, $d, d' \in D$, (unit: kWh)
TT_{ijv}	Travel time of EV v from node i to j , $v \in V$, $i, j \in I$, (unit: h)
wc_{ijv}	Remaining cargo weight of EV v from node i to j , $i, j \in I$, $v \in V$, (unit: kg)
l_{ij}	Distance from node i to j , $i, j \in I$
$L_{dd'}$	Distance from depot d to d' , $d, d' \in D$
DT_{jv}	Departure time of EV v from node j , $j \in I$, $v \in V$
LT_{dt}	Departure time of ET t from depot d , $d \in D$, $t \in TR$
AT_{jv}	Arrival time of EV v at node j , $j \in I$, $v \in V$
GT_{dt}	Arrival time of ET t at depot d , $d \in D$, $t \in TR$
JT_{ijv}	Travel time of EV v from node i to j , $i, j \in I$, $v \in V$
WT_{jv}	Waiting time of EV v at node j , and the waiting time indicates the time required to wait for the service to start. $j \in I$, $v \in V$
CT_{jv}	Charging time of EV v at CS j , $j \in R$, $v \in V$
q_j	Demand quantity of customer j , $j \in C$
u_d	Demand quantity of depot d , $d \in D$
$U_{dd'}$	Transport quantity from depot d to d' , $d, d' \in D$
LE_{iv}	Amount of energy remaining when EV v leaves node i , $i \in I$, $v \in V$
AE_{iv}	Amount of energy remaining when EV v arrives node i , $i \in I$, $v \in V$
RE_{jv}	Amount of energy remaining of EV v at node j , $j \in I$, $v \in V$
$[m_d, n_d]$	Time window for depot d , $d \in D$
$[g_c, h_c]$	Service time window for customer c , $c \in C$
Decision variable	Description
x_{dv}	If EV v travels from depot d , $x_{dv} = 1$; otherwise, $x_{dv} = 0$, $d \in D$, $v \in V$
y_{dt}	If ET t travels from depot d , $y_{dt} = 1$; otherwise, $y_{dt} = 0$, $d \in D$, $t \in TR$

Table 4 (continued)

Set	Description
x_{ijv}	If EV v travels from node i to node j , $x_{ijv} = 1$; otherwise, $x_{ijv} = 0$, $i, j \in I$, $v \in V$
$y_{dd't}$	If ET t travels from depot d to d' , $y_{dd't} = 1$; otherwise, $y_{dd't} = 0$, $d, d' \in D$, $t \in TR$
$O_{dj'}$	If customer j is reassigned from depot d to d' , $O_{dj'} = 1$; otherwise, $O_{dj'} = 0$, $d, d' \in D$, $j \in C$
k_{jv}	If EV v charged at CS j , $k_{jv} = 1$; otherwise, $k_{jv} = 0$, $j \in R$, $v \in V$

are defined and shown in [Table 4](#). In addition, several reasonable assumptions of the optimization model based on the fundamental assumptions in traditional EVRP and MDVRP are described as follows:

Assumption 1. The demands, locations, and time windows of customers are known, and the service time is ignored and the same for all customers.

Assumption 2. The EVs are homogeneous and travel at a constant speed.

Assumption 3. EVs depart from depots or CSs with full battery, and the departure time of the EVs from the depot is determined according to the service start time of the first customer on the visit route.

Assumption 4. Each CS can be used once in each EV route, and each CS can be shared by multiple EV routes.

Assumption 5. EVs can be charged at any energy level, and the charging time of EVs has a linear relationship with the amount of required electricity.

4.2. Model formulation

The energy consumption of EVs can be integrated into the model of EVRP ([Zhang et al., 2018](#); [Kucukoglu et al., 2021](#)), while the driving of EVs requires gram resistance (friction resistance, resistance and rolling resistance) to do work ([Kanchala & Ramadurai, 2020](#); [Basso, Kulcsár, & Sanchez-Diaz, 2021](#)). The involved computational formulas of θ_{ijv} , TT_{ijv} , and φ_{ijv} are presented as Eqs. (1), (2), and (3), respectively.

$$\theta_{ijv} = \frac{[(a_v + g \cdot \sin\theta + g \cdot \lambda_v \cdot \cos\theta) \cdot (wv_v + wc_{ijv}) + 0.5\sigma A_v \rho \cdot SV_v^2] \cdot SV_v}{\zeta_v} \quad (1)$$

$$TT_{ijv} = \frac{l_{ij}}{SV_v} \quad (2)$$

$$\varphi_{ijv} = TT_{ijv} \cdot \theta_{ijv} = \frac{[(a_v + g \cdot \sin\theta + g \cdot \lambda_v \cdot \cos\theta) \cdot (wv_v + wv_{ijv}) + 0.5\sigma A_v \rho \cdot SV_v^2] \cdot SV_v \cdot l_{ij}}{\zeta_v \cdot SV_v} \quad (3)$$

where the arc specific coefficient is $\delta_v = \frac{a_v + g \cdot \sin\theta + g \cdot \lambda_v \cdot \cos\theta}{\zeta_v}$, and the total weight of EV v from node i to j is $wv_v + wc_{ijv}$, which is the weight of EV v plus the remaining cargo weight of EV v from node i to j . In addition, vehicle specific coefficient is $\beta_v = \frac{0.5\sigma A_v \rho}{\zeta_v}$. Furthermore, Eq. (3) can be rewritten as Eq. (4). Therefore, the electricity consumption is calculated based on the electricity consumption of the arcs, and the route is composed of arcs, which can be said that the electricity consumption changes with the change of the route.

$$\varphi_{ijv} = [\delta_v (wv_v + wc_{ijv}) + \beta_v \cdot SV_v^2] \cdot l_{ij} \quad (4)$$

A bi-objective nonlinear optimization model including the minimization of the total operating cost and the number of used EVs is proposed to solve the CMEVRPTW-SCS. The cost objective function is established in Eq. (5), which contains five components, namely, Z_1 , Z_2 , Z_3 , Z_4 , and Z_5 . The EV objective function is described as Eq. (6).

$$M \text{ in } Z = Z_1 + Z_2 + Z_3 + Z_4 + Z_5 \quad (5)$$

$$\text{Min} \quad V = \sum_{i \in D} \sum_{j \in C} \sum_{v \in V} x_{ijv} \quad (6)$$

In Eq. (7), Z_1 is the electric delivery cost (EDC) consisting of two components: $f_e \cdot \sum_{v \in V} \sum_{i,j \in I, i \neq j} \varphi_{ijv} \cdot x_{ijv}$ is the delivery cost generated by EVs traveling between depots and customers. $FV_v \cdot \sum_{v \in V} \sum_{d \in D} x_{dv}$ represents the rental cost of EVs.

$$Z_1 = f_e \cdot \sum_{v \in V} \sum_{i,j \in I, i \neq j} \varphi_{ijv} \cdot x_{ijv} + FV_v \cdot \sum_{v \in V} \sum_{d \in D} x_{dv} \quad (7)$$

In Eq. (8), Z_2 is the facility operating cost (FOC) including two components: $\sum_{d \in D} F_d$ expresses the fixed cost of depots, and $\sum_{d \in D} \mu_d \times u_d$ is the variable cost of depots in the collaborative network.

$$Z_2 = \sum_{d \in D} F_d + \sum_{d \in D} \mu_d \times u_d \quad (8)$$

In Eq. (9), Z_3 is the penalty cost (PC) of earliness or delay when EVs arrive at customers.

$$Z_3 = PE_e \cdot \sum_{c \in C} \text{Max}(h_c - \sum_{v \in V} AT_{cv}, 0) + PL_t \cdot \sum_{c \in C} \text{Max}(\sum_{v \in V} AT_{cv} - g_c, 0) \quad (9)$$

In Eq. (10), $\psi_{dd't}$ expresses the energy consumption of ETs, and can be similarly calculated as Eq. (4). Furthermore, Z_4 denotes the centralized transportation cost caused by the sharing of customer service in Eq. (11), where $f_e \cdot \sum_{t \in T} \sum_{d,d' \in D} \psi_{dd't} y_{dd't}$ represents the transportation cost among multiple depots, and $FT_t \cdot \sum_{d \in D} \sum_{t \in T} y_{dt}$ indicates the rental cost of ETs. In other words, customer service sharing is considered in the process of centralized transportation of goods between multiple depots.

$$\psi_{dd't} = [\ell_t(wt_t + \sum_{j \in C} O_{dj'd} \cdot q_j) + \tau_t \cdot ST_t^2] \cdot L_{dd'} \quad (10)$$

$$Z_4 = f_e \cdot \sum_{t \in T} \sum_{d,d' \in D} \psi_{dd't} \cdot y_{dd't} + FT_t \cdot \sum_{d \in D} \sum_{t \in T} y_{dt} \quad (11)$$

The charging time of EVs can be calculated by Eq. (12) and, Z_5 is the charging cost (CC) of EVs and it can be calculated by Eq. (13).

$$CT_{jv} = \frac{E_v - RE_{jv}}{\delta_v} \quad (12)$$

$$Z_5 = f_{ch} \sum_{v \in V} \sum_{j \in R} k_{jv} \cdot CT_{jv} \quad (13)$$

Constraints on EV distribution:

$$\sum_{v \in V} \sum_{i \in I} x_{ijv} = 1, \forall j \in C \quad (14)$$

$$\sum_{i \in I} x_{ijv} - \sum_{i \in I} x_{jiv} = 0, \forall j \in I, i \neq j, v \in V \quad (15)$$

$$\sum_{i,j \in \mathbb{E}_v, i \neq j} x_{ijv} \leq |\mathbb{E}_v| - 1, \forall v \in V \quad (16)$$

$$l_{ij} \cdot x_{ijv} \leq l_{\max}, i, j \in I, i \neq j, v \in V \quad (17)$$

$$m_d \leq DT_{dv} \leq n_d, d \in D, v \in V \quad (18)$$

$$m_d \leq AT_{dv} \leq n_d, d \in D, v \in V \quad (19)$$

$$AT_{jv} + WT_{jv} - M(1 - x_{jiv}) \leq DT_{jv}, \forall i, j \in C, i \neq j, v \in V \quad (20)$$

$$AT_{jv} + WT_{jv} + M(1 - x_{jiv}) \geq DT_{jv}, \forall i, j \in C, i \neq j, v \in V \quad (21)$$

$$AT_{jv} + CT_{jv} - M(1 - x_{jiv}) \leq DT_{jv}, \forall j \in R, i \in C, v \in V \quad (22)$$

$$AT_{jv} + CT_{jv} + M(1 - x_{jiv}) \geq DT_{jv}, \forall j \in R, i \in C, v \in V \quad (23)$$

$$\begin{aligned} & DT_{iv} + CT_{jv} \cdot k_{jv} \cdot x_{ijv} + JT_{ijv} \cdot x_{ijv} + JT_{j(i+1)v} \cdot x_{j(i+1)v} + JT_{i(i+1)v} \cdot x_{i(i+1)v} + M(1 \\ & - x_{i(i+1)v} - x_{j(i+1)v}) \geq AT_{(i+1)v}, \forall i, i+1 \\ & \in C \cup D, j \in R, v \in V \end{aligned} \quad (24)$$

$$\begin{aligned} & DT_{iv} + CT_{jv} \cdot k_{jv} \cdot x_{ijv} + JT_{ijv} \cdot x_{ijv} + JT_{j(i+1)v} \cdot x_{j(i+1)v} + JT_{i(i+1)v} \cdot x_{i(i+1)v} - M(1 \\ & - x_{i(i+1)v} - x_{j(i+1)v}) \leq AT_{(i+1)v}, \forall i, i+1 \\ & \in C \cup D, j \in R, v \in V \end{aligned} \quad (25)$$

$$\sum_{i \in D \cup C} \sum_{j \in R} q_j \cdot x_{ijv} \leq Q_v, \forall v \in V \quad (26)$$

$$LE_{iv} = E_v, \forall i \in D \cup R, v \in V \quad (27)$$

$$AE_{iv} = LE_{iv}, \forall i \in C, v \in V \quad (28)$$

$$\frac{RE_{jv}}{E_v} \geq SOC_{\min}, \forall j \in I, v \in V \quad (29)$$

$$\begin{aligned} & AE_{(i+1)v} \leq LE_{iv} + [(E_v - RE_{jv}) \cdot k_{jv} - \varphi_{ijv} \cdot x_{ijv} - \varphi_{j(i+1)v} \cdot x_{j(i+1)v}] \cdot (1 \\ & - x_{i(i+1)v}) - \varphi_{i(i+1)v} \cdot x_{i(i+1)v}, \forall i, i+1 \\ & \in C \cup D, j \in R, v \in V \end{aligned} \quad (30)$$

Constraints on centralized transportation:

$$m_d \leq LT_{dt} \leq n_d, d \in D, t \in TR \quad (31)$$

$$m_d \leq GT_{dt} \leq n_d, d \in D, t \in TR \quad (32)$$

$$\sum_{d,d' \in D} y_{dd't} \cdot q_{dd'} \leq U_t, \forall t \in TR \quad (33)$$

$$q_{dd'} = \sum_{j \in C} O_{dj'd} \cdot q_j, \forall d, d' \in D \quad (34)$$

$$DT_{dv} \geq GT_{dt} - (2 - y_{d'dt} - x_{dv}), d, d' \in D, d \neq d', t \in TR, v \in V \quad (35)$$

Binary decision:

$$x_{iv} = \{0, 1\}, i \in D, v \in V$$

$$x_{ijv} = \{0, 1\}, i, j \in I, i \neq j, v \in V$$

$$k_{jv} = \{0, 1\}, j \in R, v \in V$$

$$y_{dt} = \{0, 1\}, d \in D, t \in TR$$

$$y_{dd't} = \{0, 1\}, d, d' \in D, t \in TR$$

$$O_{dj'd} = \{0, 1\}, j \in C, d, d' \in D$$

Constraint (14) ensures that each customer can be served by a single EV from depot or customer. Constraint (15) is the flow conservation constraint. Constraint (16) is used to eliminate subtours on every route departing from depots to serve customers. Constraint (17) ensures that the length of delivery route does not exceed the maximum driving distance of EVs. Constraints (18) and (19) stipulate the departure time and return time of EVs at depots, respectively. Constraints (20) and (21) present the arrival time of EVs plus the waiting time is equal to the departure time from a customer. Constraints (22) and (23) present the arrival time of EVs plus the charging time is equal to the departure time from a CS. Constraints (24) and (25) express that the arrival time at the next customer is equal to the departure time of the previous customer plus the charging time and travel time of EVs. Constraint (26) guarantees that each EV has sufficient capacity to meet the total demand of served customers. Constraints (27)–(29) ensure that EVs never run out of energy. Constraint (27) indicates that EVs are fully charged when leaving depots or CSs. Constraint (28) ensures that the battery power level

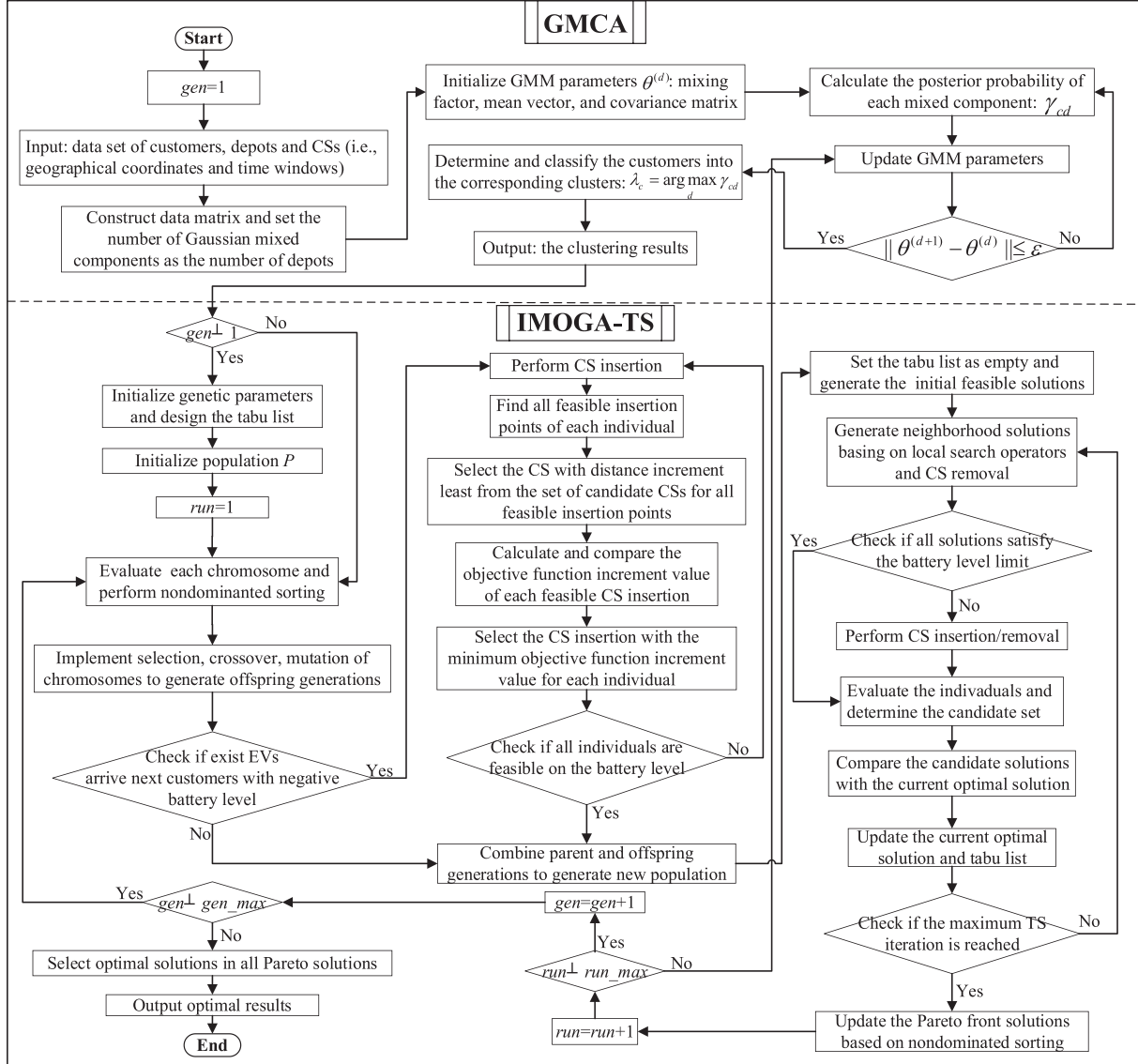


Fig. 2. Flowchart of the hybrid algorithm for CMEVRPTW-SCS optimization.

remains unchanged while EVs visit customers. Constraint (29) guarantees that each EV has sufficient battery power to complete the delivery and return to depots. Constraint (30) represents the battery energy relationship between two customers, that is, the amount of energy arriving at node $i + 1$ should not exceed the amount of energy leaving node i plus the amount charged at depots or CSs and minus the amount consumed energy in travel. Constraints (31) and (32) stipulate the departure time and return time of ETs at depots, respectively. Constraint (33) ensures that the total cargo transportation volume among depots does not exceed the capacity of ETs. Constraint (34) ensures that the amount of cargo transported is equal to the total reassigned customer demands among depots. Constraint (35) ensures that the centralized transportation among depots have been completed before starting distribution tasks.

5. Solution methodology

Heuristic algorithm is widely applied to solve large-scale logistics network optimization problems (Bae & Moon, 2016; Moghdani et al., 2021). Multi-objective genetic algorithm (MOGA) is often used to solve combinatorial optimization problems due to its high computational speed and ability to find the global optimal solution (Melo, Pereira, Reis,

Lauro, & Brandão, 2022). Meanwhile, Tabu search (TS) algorithm emphasizes on neighborhood search and searching local optima (Gmira et al., 2021). In this study, a hybrid heuristic algorithm combining GMCA with IMOGA-TS is proposed to assist in finding the optimal solution of CMEVRPTW-SCS. The detailed optimization process is shown in Fig. 2. The parameters used in the flowchart are as follows: gen denotes the number of optimization runs, gen_max is the maximum number of optimization runs, run is the count of iterations, and run_max is the maximum number of iterations.

In this study, the genetic operation, CS insertion, and non-dominated sorting are repeated in multiple iterations to obtain the Pareto front solutions. Then, the TS algorithm is incorporated to optimize the initial feasible solutions obtained from the above Pareto front. The TS operation can obtain the optimal solution by constructing extended neighboring solutions and selecting the current better solutions until the stopping condition is satisfied. Compared with traditional MOGA, two operators, namely, fast non-dominated sorting and crowding distance comparison are introduced to obtain the Pareto front and explore good individuals in the process of finding optimal routes. Moreover, CS insertion is conducted to find the best insertion point of CS for each route on the basis of the principle of minimum increment with distance and cost. The insertion and removal operators of CSs in TS are also

introduced to determine the best charging position and charging time of EVs.

5.1. Gaussian mixture clustering

Customer clustering is an important approach to simplify computation in the optimization of large-scale transportation network problems (Mesa-Arango and Ukkusuri, 2015). In the optimization model, the reassessments of customer service can be completed by customer clustering to realize the collaboration among depots. GMCA is selected to cluster customers in this study, where the classification is based on the geographical location and time window characteristics of each customer (Wang, Peng, et al., 2020).

The adopted clustering algorithm evaluates the proximity between depots and customers from three dimensions: latitude, longitude, and time windows. Customers are then assigned to the corresponding depot with a certain probability. The GMCA procedure is shown in Algorithm 1.

Input: Customer data matrix $X_c = \{x_1, x_2, x_3, \dots, x_m\}$ and depots data matrix $k_centroids$

The number of Gaussian mixed components k (the number of depots)

The number of iterations $iter_max$

Output: Customer clusters $\{\Omega_d\}_{d=1}^k$

```

1. Iter ← 0 // Initial clustering
2.  $\{\Omega_d^0\}_{d=1}^k = \emptyset$ 
3.  $\{(\alpha_d, \mu_d, Cov_d) | 1 \leq d \leq k\} \leftarrow GMM(C)$ 
4. While  $iter < iter\_max$  do // Iterated clustering
5.   For  $c = 1$  to  $m$  do // Calculate posterior probability
6.      $\gamma_{cd} \leftarrow P_M(x_c | \mu_d, Cov_d)$ 
7.   End
8.   For  $d = 1$  to  $k$  do // Update parameters
9.      $(\alpha_d', \mu_d', Cov_d') \leftarrow GMM(C)$ 
10.     $\theta^{(d+1)} - \theta^{(d)} = (\alpha_d', \mu_d', Cov_d') - (\alpha_d, \mu_d, Cov_d)$ 
11.    If  $\|\theta^{(d+1)} - \theta^{(d)}\| \leq \varepsilon$  // Check the update parameters
12.       $(\alpha_d, \mu_d, Cov_d) \leftarrow (\alpha_d', \mu_d', Cov_d')$ 
13.    End
14.  End
15. End
16. For  $c = 1$  to  $m$  do // Divide clustering
17.    $\{\Omega_{z_n}\} \leftarrow \{\Omega_{z_c}\} \cup c$ 
18. End

```

In Algorithm 1, the clustering process can be described in the following steps. First, the latitude, longitude and time windows of customers and depots are input to the construct data matrix, and the number of Gaussian mixed components are determined according to the number of depots. Second, the parameters, including mean vector, covariance matrix, and mixing factor, are initialized. Third, the posterior probability generated by each mixed component is calculated. Then, the parameters of Gaussian mixture model (GMM) are updated until the parameters become stable. Finally, the customers are determined and classified into the corresponding cluster according to the posterior probability.

GMM is conducted on the basis of the Gaussian probability density function to quantify customer characteristics accurately and achieve

customer decomposition (Mai, Fry, & Ohlmann, 2018; Jia et al., 2019). Each GMM is composed of k Gaussian distributions, and each Gaussian distribution can be regarded as a component, that is, a customer cluster. The linear addition of these clusters constitutes the Gaussian mixture distribution, which is calculated as Eq. (36).

$$P_M(x_c) = \sum_{d=1}^k \alpha_d \times P(x_c | \mu_d, Cov_d), D = \{d | 1, 2, 3, \dots, k\} \quad (36)$$

The k components of GMM correspond to k clusters. $P_M(x_c)$ is the posterior probability of customer c , which can be denoted as γ_{cd} . $P(x_c | \mu_d, Cov_d)$ is the probability density function of customer c , and x_c is the characteristics of customer c . α_d , μ_d , and Cov_d are the mixing factor, the mean vector, and the covariance matrix of cluster d , respectively. In the iterative process of GMCA, these parameters of GMM can be updated by Eqs. (37)–(39).

$$\alpha_d = \frac{\sum_{c=1}^m \gamma_{cd}}{m} \quad (37)$$

$$\mu_d = \frac{\sum_{c=1}^m \gamma_{cd} \times x_c}{\sum_{c=1}^m \gamma_{cd}} \quad (38)$$

$$Cov_d = \frac{\sum_{c=1}^m \gamma_{cd} \times (x_c - \mu_d) \times (x_c - \mu_d)^T}{\sum_{c=1}^m \gamma_{cd}} \quad (39)$$

The clustering results can be determined according to the GMM parameters, and the customers can be classified into different clusters by Eq. (40).

$$\lambda_c = \operatorname{argmax}_d \gamma_{cd} \quad (40)$$

5.2. Imoga-TS

MOGA is an intelligent evolutionary algorithm for solving multi-objective optimization problems (Owais & Osman, 2018). TS is a neighborhood search algorithm with strong local search ability, and it can avoid searching previously visited solutions by controlling memory structure and corresponding tabu criterion (Qiu, Fu, Eglese, & Tang, 2018). Therefore, we propose IMOga-TS to explore global and local solution spaces to achieve global optimization. IMOga-TS is designed to solve CMEVRPTW-SCS with the lowest cost and fewest EVs. Algorithm 2 shows the detailed optimization process (Ghannadpour & Zandiye, 2020; Wang, Li, Guan, Fan, et al., 2021).

In Algorithm 2, the optimization process consists of the following steps. First, the initial population is generated, and each individual is evaluated. Second, selection, crossover, and mutation are carried out to optimize the initial population. Third, CS insertion is executed when the battery level of EVs in the delivery routes appears negative. Forth, TS operation is performed and the neighborhood is searched to obtain the candidate solutions. Finally, the Pareto front are formed by non-dominated sorting for the candidate solutions, and the optimal solution is selected from the Rank1 solutions based on the crowding distance.

```

Input: (1) Objective function  $F(x)$ 
      (2) Population size ( $pop\_size$ )
      (3) Tabu list ( $TL$ )
      (4) Maximum iterations ( $run\_max, t\_max$ )
1.  $g \leftarrow 0$ 
2.  $P_0 \leftarrow$  Initialize random population
3. While  $run \leq run\_max$ 
4.   For population = 1:  $pop\_size$  // Generate offspring populations
5.     Evaluate ( $P_0$ )
6.      $P' \leftarrow$  Selection ( $P$ )
7.      $P'' \leftarrow$  PMX crossover ( $P'$ )
8.      $P''' \leftarrow$  Mutation ( $P''$ )
9.      $S \leftarrow P'''$  // Decode
10.    If  $T_r^Q(S) > 0$ 
11.      |  $S' \leftarrow$  Perform CS insertion ( $S$ )
12.    End
13.  End
14.  For  $t=1: t\_max$ 
15.    |  $S'' \leftarrow$  TS ( $S'$ )
16.  End
17.   $S^* \leftarrow$  Pareto dominance rank ( $S''$ )
18. End

```

5.2.1. Solution presentation and evaluation

The solution presentation plays a key role in the transformation between chromosomes and the actual routes in the iterative process of population optimization (Hermann et al., 2019). Customer sequence and charging position should be considered in the CMEVRPTW-SCS simultaneously. Each route starts at the depot, visits customer vertices, and ends at the depot. Fig. 3 shows the solution presentation.

In Fig. 3, the tour with 15 customers, a depot, and two CSs can be divided into three delivery routes. Customers are coded by 1–15, and charging stations are coded by 16–17. First, the customer sequence is

formed randomly. Second, the chromosome sequence is decoded into three EV routes according to the maximum load of EVs. Finally, CSs are inserted into the customer sequence based on the energy load constraints of EVs. The procedure of inserting CS attempts to insert the CSs between the different customers to maintain an adequate level of the battery at any point along the tour, and CS can be shared among multiple delivery routes. This rule helps to fulfill the load capacity and battery capacity of routes, but it cannot completely guarantee the occurrence of violation of the constraints. The constraint violations are defined and described as follows. Battery capacity violation refers to the energy consumption of a route is higher than the battery capacity of EVs. Load capacity violation refer to the total demand of the delivered customers on a route is greater than the capacity of the EV.

$RO(ro)$ and T_{ro} represent the set of routes and the evaluation data of each route, respectively, $ro \in RO(ro)$. T_{ro}^Q and T_{ro}^E are the load capacity violations and the energy violations of route ro , respectively. Violating constraints will be penalized with the penalty function $PF(ro)$, as shown in Eq. (41), which is defined as the combination of the objective function and the sum of all violations. M is an extremely large number, and $Z_2(ro)$ is an objective function of route ro .

$$PF(ro) = M \cdot T_{ro}^Q + M \cdot T_{ro}^E + Z_2(ro) \quad (41)$$

5.2.2. Genetic operator

The quality of individuals thoroughly depends on the selection, crossover, and mutation operators in genetic algorithm (Karakatić and Podgore, 2015; Katoch, Chauhan, & Kumar, 2021). The selection operator permits a limited number of promising chromosomes to be selected in preparation for reproducing new chromosomes (Sethanan & Jamrus, 2020). The crossover and mutation operations are the main and auxiliary operators to generate new chromosomes, respectively, which can ensure the global and local equilibrium search ability of the proposed algorithm by cooperating and competing with each other (Park, Son, Koo, & Jeong, 2021). The purpose of the two operators is to facilitate the

chromosomes after crossover or mutation become more excellent in performance. If the excellent chromosome cannot be obtained after crossover, the parent chromosome will be mutated directly. If the excellent chromosome still cannot be achieved after mutation, the parent chromosome will be retained. This means that mutation operation not always occurs after the crossover operation. All the chromosomes derived from selection, crossover, and mutation will be evaluated and compared to retain elite individuals by the Pareto ranking.

(1) Selection operator

Selection is the process of selecting parents that can be mated and recombined to create offspring for the next generation. Parent selection is crucial to the convergence rate of GA, as good parents drive individuals to better and fitter solutions (Mohammed et al., 2017; Erdem & Koç, 2019; Wang, Li, Guan, Fan, et al., 2021). Roulette wheel selection is adopted in this study to select the individuals with better fitness value and is then added to the parent population. The principle of roulette wheel selection is presented in Fig. 4.

In Fig. 4, the disk represents all the individuals, each of which has a probability of being selected and individual 3 is most likely to be selected. The probability of any individuals being selected into a new population is proportional to the fitness value of the individual. The probability PR_j can be calculated by Eq. (42), where f_j is the fitness value of individual j , and n is the total number of individuals.

$$PR_j = \frac{f_j}{\sum_{i=1}^n f_i} \quad (42)$$

(2) Crossover operator

The crossover operator generates new individuals by swapping several gene segments between two parents selected from the population. The purpose of this operator is to ensure that the traits of excellent individuals in parents can be continued and inherited in offspring individuals (Pierre & Zakaria, 2017; Park et al., 2021). Thus, new individuals created by crossover can be accepted, but they need to be further tested by fitness functions to retain good ones. For the crossover process on the parent chromosome, this study adopts a partial mapping crossover (PMX), which involves taking two chromosomes from the original population, selecting two genes on each chromosome and then

crossing them to form new ones. Fig. 5 shows the PMX process, where the natural numbers 1–15 represent customers.

The detail processes are as follows: First, randomly select the starting (e.g., genes 3 and 4) and ending positions (e.g., genes 10 and 9) of several genes in a pair of parent chromosomes. Then, swap the positions of the two groups of genes. Third, look for the correspondence of each gene in the two groups and match one to the other. Finally, establish a mapping relationship according to the two groups of genes exchanged, and detect and adjust the conflicts in the new pair of offspring genes.

(3) Mutation operator

Mutation is the process of changing a gene on a chromosome to generate a new one. The purpose of mutation is to maintain the diversity of the population by preventing them from being local optimum. (Mohammed et al., 2017). The mechanism of the mutation operator is used to change the gene values at specific loci of a chromosome in the population. In this study, the mechanism is used to change the delivery order of customers in the delivery routes. The process of mutation operator is shown in Fig. 6.

The procedure of mutation occurs before the offspring is released into the space (Owais & Osman, 2018; Katooch et al., 2021). The mutation operator is conducted on a parent chromosome by randomly selecting multiple genes, and exchanging their position to form a different chromosome. For example, the genes 13, 8, and 15 are selected from the parent chromosome, and then the three genes are swapped and regenerated among them for achieving a new chromosome. The generated new chromosome will be verified by calculating the fitness function value. If the fitness function value is superior to the chromosome before the mutation, then the new chromosome can be approved, otherwise, the new chromosome is invalid.

5.2.3. Tabu search procedure

TS is a procedure to explore the search space by moving from a solution to its best neighbor, which can increase the possibility of moving out from local optima. In this study, the TS algorithm can further optimize the initial Pareto solutions generated by genetic operation. The specific operation steps are shown in Algorithm 3.

Algorithm 3 TS

Input: (1) The Pareto feasible solutions S' obtained by the genetic operators
 (2) Tabu list (TL)
 (3) Maximum iterations (t_max)

Output: The optimal solution S^*

1. $\{\phi\} \leftarrow$ Initial tabu list TL
 2. $S' \leftarrow$ Generate the initial solutions
 3. **While** $t < t_max$ **do**
 4. // Neighborhood solutions $(S'') \leftarrow$ Local search
 5. $S'' \leftarrow$ Swap (S')
 6. $S'' \leftarrow$ Reverse (S')
 7. $S'' \leftarrow$ Insertion (S')
 8. $S'' \leftarrow$ CS removal/insertion (S')
 9. $S^* \leftarrow$ Evaluate (S'')
 10. **If** $S^* < S'$
 11. $TL \leftarrow TL \cup$ Move (S^*)
 12. $S' \leftarrow S^*$
 13. **End**
 14. Update S^* and TL
 15. **End**
-

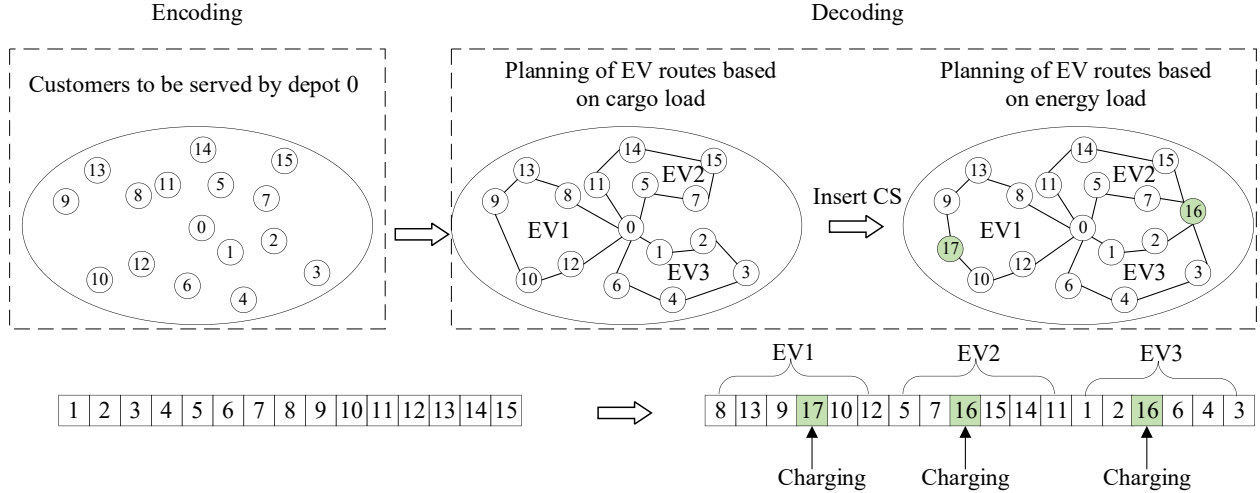


Fig. 3. Presentation of solutions.

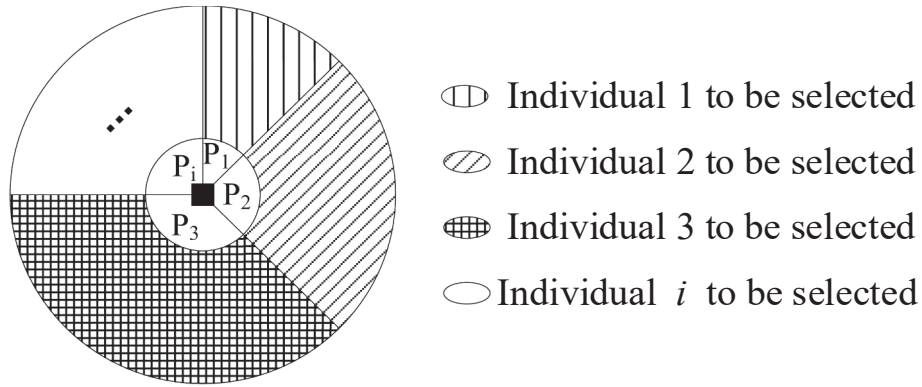


Fig. 4. Roulette wheel selection method.

In Algorithm 3, the initial feasible solution S' is generated from the Pareto front. First, the tabu list is set to empty. Then, the composite neighborhood solutions are generated by local operators (i.e., swap,

reverse, insert, and remove). Third, the objective function is evaluated to determine the candidate set, and the optimal solution S^* is compared with the initial solution S' . Finally, the optimal solution S^* and tabu list

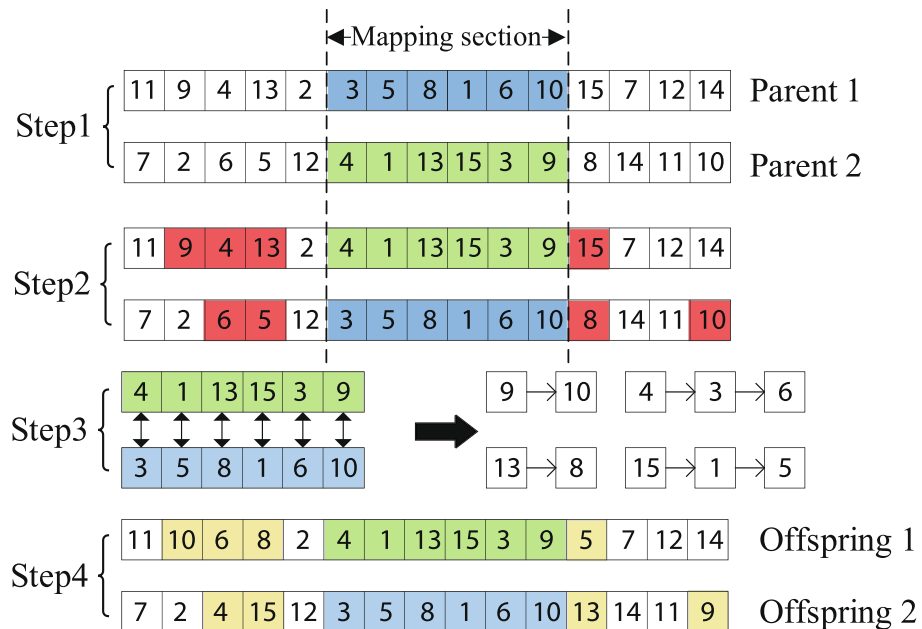


Fig. 5. PMX crossover procedure.

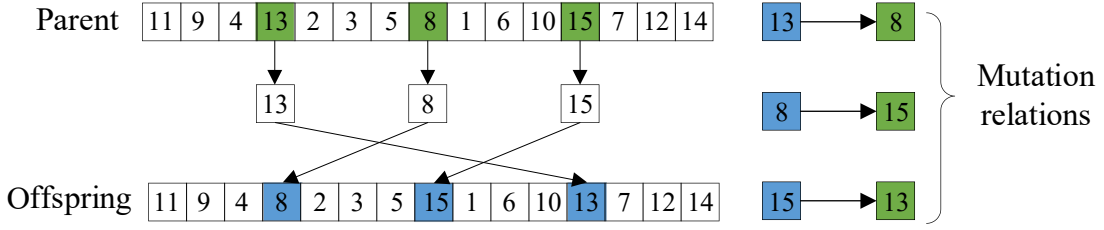


Fig. 6. Mutation operator.

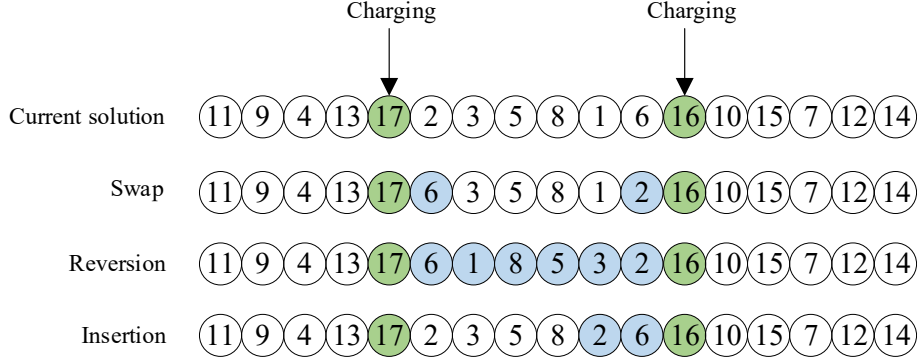


Fig. 7. Local search operators of customers.

are updated.

The TS algorithm is widely used to find the optimal solution because of its local search method (Soto et al., 2017; Goeke, 2019). Local search changes the customer visited sequences only if a better solution is available, that is, the customer visited sequence of the selected individual is changed to find the optimal route (Karakatić & Podgorelec, 2015). Considering the characteristics of CMEVRPTW-SCS, three types of local search operators for customers are designed to generate potential solutions (Wang, Li, Guan, Fan, et al., 2021). The detailed interpretation of the three types of operators is shown in Fig. 7.

In Fig. 7, the three types of operators adopted to generate the neighborhood solutions are as follows: (a) customer swap: select two customers (node 2 and node 6) and swap their positions; (b) customer reversion: select two customers (node 2 and node 6) to swap their

positions and arrange the other customers in the two customers in reverse order; (c) customer insertion: select two customers and insert one (node 2) in front of the other (node 6).

The tabu list is adopted to escape from local optima during the local search procedure by storing move information of the local search operations. The node information changes in the move and the used local search procedure information will be stored in the tabu list to prohibit the same move for several iterations, and avoid recreating a solution that is the same to the previous one. In addition, the aspiration criterion of TS is considered for the tabu list, that is, a move that is declared tabu will still be accepted if it provides a better solution. The length of the tabu list is controlled by the parameter TL . If the tabu list length exceeds TL , the oldest information in the tabu list will be deleted (Küçükoglu, Dewil, & Dirk, 2019).

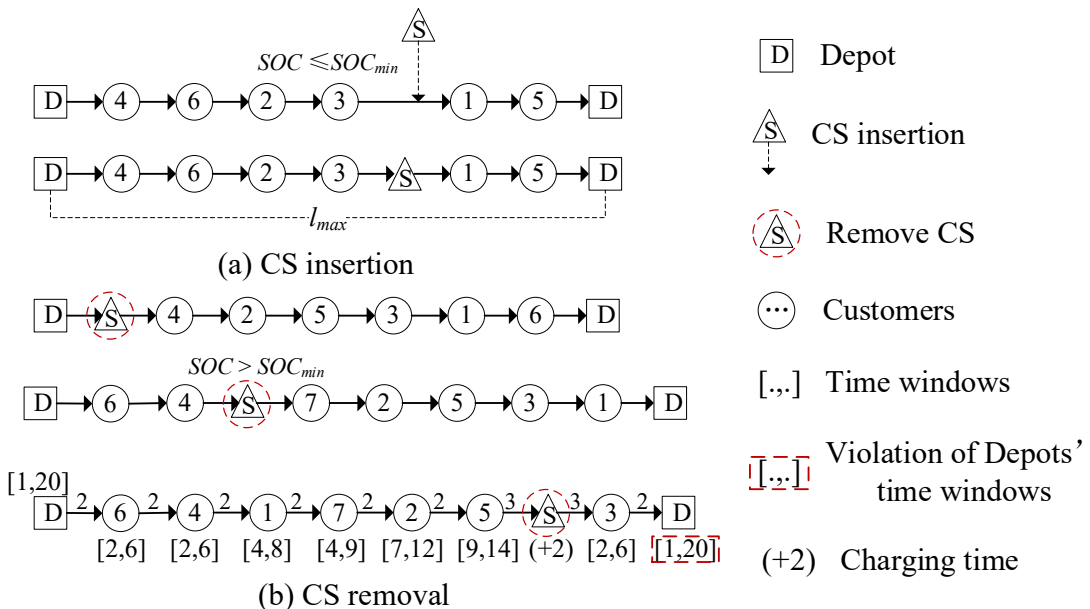


Fig. 8. CS insertion/removal.

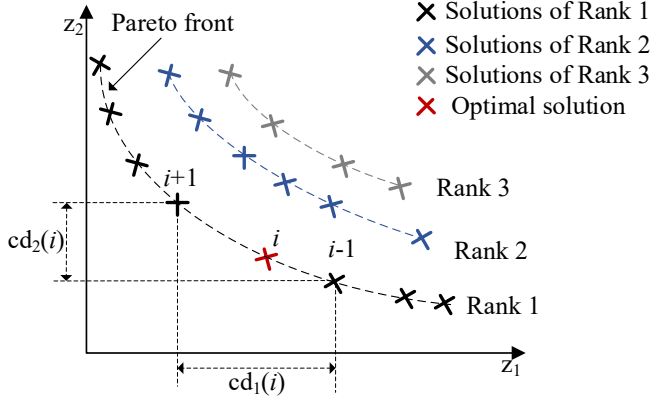


Fig. 9. Optimal solution acquisition process from the Pareto front.

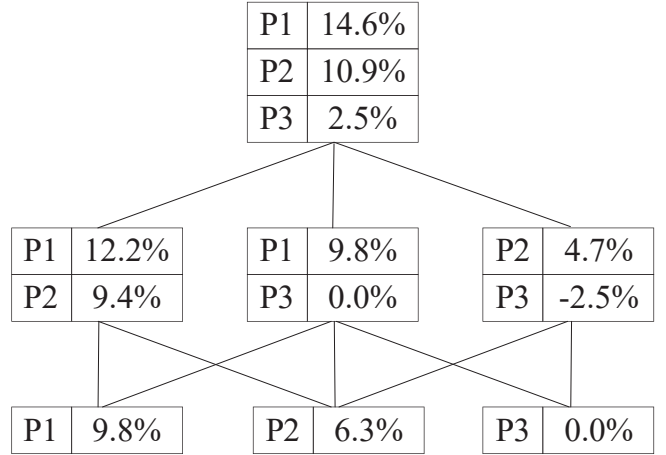


Fig. 10. Cost reduction percentages of the three-participant example.

Table 5
Parameters and description used in the Shapley value model.

Parameter	Description
N	The set of all participants, $N = \{1, 2, \dots, n\}$.
B	The subsets of N , $B \subseteq N$.
σ	The synergy coefficient of the organizer to coordinate the collaboration.
$C_0(n)$	Costs of n without coalition, $n \in B$.
$C(B)$	The total cost of alliance B .
$P(B - \{n\})$	The remaining profit of alliance B excluding participant n .
$\varphi_n(N, P)$	The allocated profit of participant n in alliance N
$\pi(s)$	The rank of member s in sequence π .
$\eta(n, \pi, s)$	The cost reduction percentage of member n in the sequence π when the s th member joins the alliance

5.2.4. CS insertion/removal

CSs are the crucial components of the proposed CMEVRPTW-SCS. Changing the positions of CSs in the visit sequence of a delivery route may improve the solution. In a pre-determined number of iterations, CS insertion/removal procedure is applied to guarantee that the battery level of EVs is adequate in a delivery route (Schneider et al., 2014; Keskin & Çatay, 2016; Hiermann et al., 2019). The specific removal and insertion operators are shown in Fig. 8. The detailed CS insertion procedure of a route is as follows:

Step 1: Evaluate the route to identify the first customer at which the EV arrives with a negative battery level.

Step 2: Insert a CS on the arc between that customer and the previous one. Then, the previous arcs are attempted in the same manner until all the feasible insertion points are found.

Step 3: Calculate the sum of distances from each CS to the previous customer and the next customer for all feasible insertion points obtained by Step 2.

Step 4: Compare the distance obtained in Step 3, and select the corresponding CS with the minimum distance to each feasible point for insertion.

Step 5: Calculate the cost increment for each feasible CS insertion obtained in Step 4.

Table 6
An assumptive three-participant example.

Alliances	$\sum_{n \in N} C_0(n)$	$C(n)$	$P(n)$	$\varphi(N, P)$
{P1}	410	370	40	(40; •; •)
{P2}	320	300	20	(•; 20; •)
{P3}	200	220	0	(•; •; 0)
{P1, P2}	730	650	80	(50; 30; •)
{P1, P3}	610	570	40	(40; •; 0)
{P2, P3}	520	510	10	(•; 15; -5)
{P1, P2, P3}	930	830	100	(60; 35; 5)

Step 6: Compare the cost increment obtained in Step 5, and select the insertion point corresponding to the least cost increment to insert CS.

In Fig. 8(a), one CS is inserted into C1 and C2. The CS insertion will be executed if the battery level of EVs in the delivery routes reach a set value. That is, the state of charge (i.e., SOC) of EVs reach the minimum SOC (i.e., SOC_{min}). Meanwhile, the distance of delivery route (i.e., l) cannot exceed the maximum delivery distance (i.e., l_{max}) after inserting CS in the delivery route (Keskin & Çatay, 2016; Hiermann et al., 2019). SOC_{min} refers to the lower bound of state of charge set to avoid range anxiety of EVs, and l_{max} is the upper bound of the driving range of EVs. Since the CS sharing strategy is implemented, all CSs are always available, and any CS can be inserted through the CS insertion operator. Fig. 8(b) presents three situations in which CSs can be removed as follows. (1) The CS can be removed from the route when the EV can still visit the following customers in the given sequence without CSs; (2) The CSs have a relatively high SOC will be removed, that is, the SOC of EV does not reach the SOC_{min} ; (3) The CS should be removed if the EV cannot return to the depot within the specified time window.

5.2.5. Pareto ranking in IMOGA-TS

The final goal of a multi-objective optimization algorithm is to identify solutions in the Pareto optimal set, which can be achieved by Pareto ranking and crowding distance calculation (Long et al., 2019; Melo et al., 2022). The Pareto ranking method refers to the ordering of individuals in a population according to their non-dominant relationships. We assume that $n(i)$ is the number of solutions that dominate individual i , and $S(i)$ is the set of solutions dominated by individual i . The detailed procedure of non-dominated sorting is summarized as follows:

Step 1: All individuals with $n(i) = 0$ in the population (all the individuals in the population that are not dominated by other individuals) are found and placed in the current set $F(1)$, where $F(1)$ denotes the first rank.

Step 2: For each individual j in the current set $F(1)$, the set $S(j)$ of individual j dominates is investigated, $n(j) = n(j)-1$.

Step 3: If $n(j)-1 = 0$, the individual j is deposited into another set $F(2)$. $F(2)$ is regarded as the set of second-level non-dominated individuals, and the individuals in this set are given the same non-dominated ranking 2 (Rank 2).

Step 4: Repeat the operations in Step 3 until the entire individuals is ranked.

The non-dominated set is the Pareto front, and the equivalent solutions of the Pareto front have the same degree of optimization. If two individuals have different non-dominated rankings, the individual with the smaller rank number is selected. If two individuals are in the same level, the one that is less crowded is selected. Fig. 9 illustrates the

Table 7

Possible sequential alliances for grand alliance.

$\pi_1 = \{P1, P2, P3\}$	P1	P2	P3	$\pi_2 = \{P2, P1, P3\}$	Participant n	P2	P1	P3
$\eta(n, \pi, 1)$	9.8 %	—	—	$\eta(n, \pi, 1)$	6.3 %	—	—	—
$\eta(n, \pi, 2)$	12.2 %	9.4 %	—	$\eta(n, \pi, 2)$	9.4 %	12.2 %	—	—
$\eta(n, \pi, 3)$	14.6 %	10.9 %	2.5 %	$\eta(n, \pi, 3)$	10.9 %	14.6 %	2.5 %	—

Table 8

Characteristics of the data instances.

Instances	Datasets	Number of depots	Number of customers	Vehicle capacity	Number of CSs
1	4D_10CS_1	4	48	200	10
2	4D_10CS_2	4	96	195	10
3	4D_10CS_3	4	144	190	10
4	4D_10CS_4	4	192	185	10
5	4D_10CS_5	4	240	180	10
6	4D_10CS_6	4	288	175	10
7	6D_14CS_1	6	72	200	14
8	6D_14CS_2	6	144	190	14
9	6D_14CS_3	6	216	180	14
10	6D_14CS_4	6	288	170	14
11	4D_10CS_7	4	48	200	10
12	4D_10CS_8	4	96	195	10
13	4D_10CS_9	4	144	190	10
14	4D_10CS_10	4	192	185	10
15	4D_10CS_11	4	240	180	10
16	4D_10CS_12	4	288	175	10
17	6D_14CS_5	6	72	200	14
18	6D_14CS_6	6	144	190	14
19	6D_14CS_7	6	216	180	14
20	6D_14CS_8	6	288	170	14
21	8D_20CS_1	8	96	200	20
22	8D_20CS_2	8	192	195	20
23	8D_20CS_3	8	288	190	20
24	8D_20CS_4	8	384	185	20
25	8D_20CS_5	8	480	180	20
26	8D_20CS_6	8	576	175	20
27	12D_28CS_1	12	144	200	28
28	12D_28CS_2	12	288	190	28
29	12D_28CS_3	12	432	180	28
30	12D_28CS_4	12	576	170	28

procedure of obtaining the Pareto optimal solution at the Pareto front.

As shown in Fig. 9, the solutions in different Pareto fronts are calculated by objectives Z_1 and Z_2 . The optimal solution can be obtained by sorting the solutions from Rank 1 in accordance with their crowding distances. The calculation of crowding distance aims to obtain solutions along the Pareto front without using a fitness sharing parameter (Ghannadpour & Zandiyeh, 2020; Melo et al., 2022). The crowding distance of individual i in the function k can be calculated as Eq. (43).

$$cd_k(i) = \frac{z_k(i+1) - z_k(i-1)}{z_k^{\max} - z_k^{\min}} \quad (43)$$

where $i+1$ and $i-1$ are two adjacent solutions on the same front; z_k^{\max} and z_k^{\min} represent the maximum and minimum values of the objective

function κ , respectively. Then, the crowding distance of solution i can be calculated as the sum of distance in κ objective functions by using Equation (44).

$$cd(i) = \sum_{k=1}^K cd_k(i) \quad (44)$$

The crowding distances of the solutions in the same non-dominated front are compared, and the solution with a higher crowding distance is the winner, in other words, the individual with the largest crowding distance in Rank 1 will be selected as the optimal solution.

5.3. Profit allocation

5.3.1. Shapley value model

In CMEVRPTW-SCS, customers are served by depots that are allocated through clustering. Thus, the depots cooperate with one another, and a fair method of profit distribution is required to stabilize this cooperation (Wang et al., 2018). All alliance participants expect to be reasonably rewarded for their contributions. The Shapley value model is an effective profit distribution mechanism based on the participants' contributions (Wang et al., 2017; Jouida et al., 2021). The cost savings (i.e., profits) from the CMEVRPTW-SCS optimization can be calculated from a non-optimal network structure to an optimal one and served as an input to allocate profit among multiple depots. Furthermore, CS sharing, customer service sharing, and centralized transportation demands are integrated to minimize the total operating cost of the CMEVRPTW-SCS optimization. The definition of parameters related to profit distribution in this study is shown in Table 5.

$P(B)$ indicates the profits of alliance B and can be calculated by Eq. (45). To achieve the fundamental purpose of the alliance and to gain more profits, the collaborative coefficient σ is introduced into the Shapley value model. The greater σ value is, the greater benefits alliance organizers obtain. Meanwhile, alliance participants gain fewer benefits. The alliance can only be formed if the participation of one member results in more cost savings. Otherwise, $P(B)$ will be set to 0. The allocated profit of a participant in alliance can be obtained from Eq. (46). $P(B) - P(B - \{n\})$ indicates the marginal contribution of participant n to alliance N . Furthermore, the cost reduction percentage can be calculated by Eq. (47).

$$P(B) = (1 - \sigma) \max \left\{ \sum_{n \in B} C_0(n) - C(B), 0 \right\} \quad (45)$$

$$\varphi_n(N, P) = \sum_{B \subset N, n \in N} \left[\frac{(|B| - 1)! (|N| - |B|)!}{|N|!} \right] \times [P(B) - P(B - \{n\})] \quad (46)$$

$$\eta(n, \pi, s) = \frac{\varphi_n(\cup_{\pi(b) \leq s, b \in N} b, P)}{C_0(n)}, s \geq \pi(n) \quad (47)$$

When a collaborative alliance is established, the collaborative members will receive additional profit, which will be regarded as the incentive for the concerned member to maintain the collaboration. The sequence in which participants join the alliance will affect the stability of the alliance. The cost reduction percentage per member when a new participant joins an alliance is adopted to measure the stability of the alliance. To sum up, the Shapley value model allocates the additional profit to each participant according to their contributions for ensuring

Table 9

Parameters used in the four algorithms.

Parameters used in the four algorithms	
MOGA	Population size: $popsize = 100$
NSGA-II	Selection probability: $ps = 0.5$
IMOOGA-TS	Crossover probability: $pc = 0.8$
MOHSA	Mutation probability: $pm = 0.2$ Harmony memory size: $HMS = 20$ Harmony memory considering rate: $HMCR = 0.7$
Other Parameters	Pitch adjusting rate: $PAR = 0.5$ Minimum state of charge: $SOC_{\min} = 25\%$ Maximum distance: $l_{\max} = 100$

Table 10

Comparison results of the three algorithms.

Instance	IMOGA-TS				MOGA				NSGA-II				MOHSA			
	Cost (\$)	EVs	CSs	COT (s)	Cost (\$)	EVs	CSs	COT(s)	Cost (\$)	EVs	CSs	COT(s)	Cost (\$)	EVs	CSs	COT(s)
1	3548	4	9	192	4425	9	9	212	4263	9	9	226	4390	8	9	233
2	3904	8	8	219	4167	11	10	237	3800	8	9	247	4039	9	10	250
3	4148	13	8	230	5024	15	10	246	4980	14	9	254	5097	14	9	260
4	4408	20	8	226	4883	22	9	239	4700	22	9	247	4843	22	9	259
5	4678	24	8	235	5329	29	10	242	5210	26	9	257	5310	27	8	266
6	5108	29	8	242	5936	33	10	249	5813	30	9	264	5908	31	9	274
7	4857	6	12	246	5187	10	13	254	4802	6	13	271	5038	8	13	282
8	5400	14	10	275	6302	15	14	283	6184	14	13	303	6293	14	13	318
9	6023	21	10	289	6587	25	13	302	6499	24	12	314	6601	24	13	329
10	6357	30	12	296	6935	31	13	309	6856	28	13	323	6978	29	13	332
11	3693	4	8	204	4262	5	10	207	4205	4	9	227	4255	4	10	236
12	4007	9	9	224	4572	10	9	234	4455	7	9	251	4610	9	9	258
13	4305	13	9	239	4942	17	10	244	4834	17	9	261	4915	17	9	276
14	4511	20	8	236	5001	21	9	241	4911	18	9	256	5003	20	9	265
15	4912	24	8	249	5582	25	9	263	5467	22	9	280	5586	23	9	285
16	5166	30	8	261	5391	35	10	273	5198	33	9	286	5333	33	9	297
17	4859	6	12	276	5322	10	13	295	5146	9	13	304	5259	10	13	318
18	5483	15	12	279	6197	20	13	284	6082	18	12	303	6188	18	12	310
19	6131	21	11	294	6802	26	13	314	6625	24	12	326	6794	25	12	338
20	6682	29	10	292	7528	31	13	298	7435	30	12	308	7557	30	13	310
21	7157	9	18	221	7407	14	18	242	7213	12	18	252	7328	12	18	254
22	7829	20	17	230	8627	21	19	250	8467	18	18	268	8612	20	19	283
23	8339	29	18	293	8690	33	19	302	8541	33	19	321	8627	34	19	329
24	8801	38	15	352	9352	42	19	363	9312	40	18	386	9348	41	18	388
25	9481	49	18	393	9997	53	18	419	9957	52	18	433	10,025	52	18	437
26	10,208	58	16	447	11,029	63	18	451	10,927	61	17	469	11,065	62	18	476
27	9671	12	24	263	10,128	15	27	284	10,054	12	26	297	10,134	14	27	309
28	10,792	24	24	346	11,222	28	27	362	11,088	28	26	379	11,205	28	26	390
29	12,004	40	25	379	12,695	45	27	398	12,522	42	26	409	12,673	43	27	411
30	12,859	55	24	471	13,303	58	27	476	13,195	57	26	488	13,305	57	26	492
Average	6511	22	13	280	7094	26	15	292	6958	24	14	307	7077	25	14	316
p-value					1.98E-16	1.19E-12	1.05E-09	7.56E-12	2.60E-11	2.67E-04	2.86E-08	1.32E-21	1.87E-14	5.77E-08	4.09E-08	2.59E-22

the stability of the alliance.

5.3.2. Profit allocation application with Shapley value model

After the optimization of the EV distribution network via the proposed hybrid algorithm, the total cost savings can be calculated and profits can be allocated among depots from nonempty alliances to generate the optimal profit allocation strategy. Table 6 shows the

calculation procedure of an assumptive three-participant example to practice the Shapley value model. Assume $\sigma = 0$ for convenience of calculation.

In Table 6, all the possible alliances are listed and the profits obtained from cost savings are allocated to each participant of alliance based on the Shapley value model. In order to further evaluate the impact of the implementation of the collaboration mechanism and the

Table 11
Results of three indicators for IMOGA-TS, MOGA, NSGA-II, and MOHSA.

Instance	IMOGA-TS			MOGA			NSGA-II			MOHSA		
	HV	NOP	MID	HV	NOP	MID	HV	NOP	MID	HV	NOP	MID
1	0.83	12	3672.15	0.75	9	3869.21	0.81	11	3714.31	0.78	10	3772.36
2	0.72	9	4013.21	0.68	10	4523.06	0.71	10	4225.16	0.70	8	4368.29
3	0.69	9	4362.52	0.57	8	4587.19	0.68	9	4478.25	0.61	9	4498.75
4	0.79	11	4528.79	0.62	9	5015.71	0.71	11	4637.43	0.65	9	4825.41
5	0.65	10	4718.26	0.59	10	5338.35	0.65	11	4901.57	0.63	11	5134.64
6	0.81	9	5304.12	0.78	8	6027.18	0.82	9	5416.81	0.79	9	5633.52
7	0.83	8	5122.08	0.73	8	5782.63	0.75	9	5193.54	0.75	8	5382.81
8	0.87	10	5537.71	0.69	9	6355.87	0.73	10	5652.38	0.71	10	5976.57
9	0.91	12	6132.41	0.79	8	7126.34	0.76	8	6249.18	0.79	9	6839.35
10	0.72	13	6723.55	0.65	11	7528.25	0.79	12	6845.29	0.68	10	7152.59
11	0.75	11	3861.92	0.58	10	4362.82	0.68	11	3946.52	0.62	11	4234.85
12	0.80	10	4107.28	0.71	8	4411.32	0.73	10	4307.16	0.73	10	4358.16
13	0.76	11	4457.17	0.72	7	4890.75	0.78	9	4548.73	0.73	8	4673.23
14	0.92	12	4593.39	0.83	10	5025.49	0.82	8	4717.65	0.85	11	4869.51
15	0.85	11	5162.41	0.72	9	5873.27	0.76	10	5285.82	0.75	10	5528.39
16	0.86	10	5324.86	0.75	9	6235.68	0.71	9	5238.45	0.73	9	5714.85
17	0.91	12	4936.52	0.78	10	5691.32	0.79	10	4972.18	0.76	11	5416.72
18	0.83	10	5570.63	0.81	8	5876.29	0.75	9	5563.27	0.72	10	5998.16
19	0.81	13	6308.22	0.67	9	7125.51	0.78	10	6306.51	0.81	9	6527.89
20	0.85	12	6741.75	0.72	8	7864.72	0.82	11	6778.64	0.78	10	6983.52
Average	0.81	10.75	5058.95	0.71	8.9	5675.55	0.75	9.85	5148.94	0.73	9.6	5394.48

Table 12

Comparison results of four indicators among four algorithms.

Algorithms	Performance measures		
	HV	NOP	MID
IMOGA-TS	0.81	10.75	5058.95
MOGA	0.71	8.9	5675.55
NSGA-II	0.75	9.85	5148.94
MOHSA	0.73	9.6	5394.48

charging station sharing strategy on the EV distribution network, the cost reduction percentage of each participant among various alliances can be calculated and analyzed in Fig. 10.

As shown in Fig. 10, the negative cost reduction percentage of P3 in the collaboration with P2 indicates that P3 will not accept the collaborative alliance. The synergy among multiple participants is mainly to seek profit maximization. However, the difference of alliance sequences will lead to the difference of profit distribution scenarios and affect the stability of the grand alliance. Thus, the possible sequential combinations on profit distribution are analyzed and shown in Table 7.

In Table 7, $\pi_1 = \{P1, P2, P3\}$ and $\pi_2 = \{P2, P1, P3\}$ are the only two appropriate sequences meeting the Strictly monotonic path (SMP) principle (Wang et al., 2017; Wang, Li, Guan, Xu, et al., 2021), due to their cost reduction percentages increase when each participant joins the alliance. Based on diagonal maximal lowest rule of SMP method, the minimum cost reduction percentages for π_1 and π_2 on the diagonal both are equal to 2.5 %, and then the second smallest percentage on the diagonal are selected. The cost reduction rate of π_1 when P1 joins reaches 9.8 %, while this rate of π_2 is only 6.3 % when P2 joins. Thus, the most favorable sequence of $\pi_1 = \{P1, P2, P3\}$ is selected as the optimal profit allocation strategy.

6. Implementation and analysis

6.1. Algorithm comparison

In this section, the proposed algorithm is compared with MOGA (Pierre & Zakaria, 2017), non-dominated sorting genetic algorithm-II (NSGA-II) (Rabbani, Farrokhi-Asl, & Asgarian, 2016), and multi-objective harmony search algorithm (MOHSA) (Yassen, Ayob, Nazri, & Sabar, 2017) to test the effectiveness and superiority of IMOGA-TS in solving CMEVRPTW-SCS. A total of 30 benchmark instances for the algorithm comparison is constructed on the basis of the dataset (i.e., multidepot VRP with time windows (MDVRPTW)) of the NEO Research Group database.¹ CMEVRPTW-SCS contains two types of charging facilities (i.e., Depots and CSs), and the locations of the CSs are randomly selected from customer locations. For example, the 10 CSs in Instance 1 are randomly selected from the 48 customers in the same instance. The remaining data characteristics of Instances 1–20 in CMEVRPTW-SCS are consistent with the MDVRPTW database. Meanwhile, Instances 21–30 is the combination of Instances 1–10 and 11–20. Table 8 shows the specified characteristics of the modified instances in each column, including the number of depots, the number of customers, EV loading capacity, and the number of CSs.

Based on the CMEVRPTW-SCS datasets given in Table 8, a comparison of the proposed IMOGA-TS with MOGA, NSGA-II and MOHSA is performed. The CS insertion operator is integrated into the four algorithms and used to execute these 30 instances shown in Table 8. In MOGA, the CSs are inserted into delivery routes after the mutation operation to obtain the energy feasible optimization solution (Long et al., 2019). In NSGA-II, CS insertion operation is performed after the Pareto ranking to complete the construction of excellent solutions

Table 13

Initial characteristics of logistics facilities.

Depots	Customers	Number of customers	CSs
D1	C1-C33	33	CS1, CS3, CS4, CS11
D2	C34-C73	40	CS6, CS8, CS9, CS13
D3	C74-C111	37	CS5, CS7, CS12
D4	C112-C143	32	CS2, CS10

(Wang, Zhe, et al., 2022). In MOHSA, the CS insertion operator is executed by check the battery level of EV in the delivery route after the new harmony generated and before the harmony memory updated (Chen, Chen, & Gao, 2017). The specific parameters of four algorithms and EVs are listed in Table 9. Each of the four algorithms is executed 20 times based on the modified data instance, and the optimal solution is selected as the final calculation results for each algorithm. The total operational cost (TOC), number of EVs (EVs), number of used CSs (CSs), and computation time (COT) are calculated by the proposed four algorithms based on the collaboration mechanism, integrating centralized transportation, CS sharing, and customer service sharing are shown in Table 10.

In Table 10, the significant differences in the *p*-value based on paired double sample mean analysis for the algorithm comparison indicate that the analysis based on the four algorithms is reasonable. First, except for Instances 2 and 7, the cost of IMOGA-TS is completely lower than the cost calculated by the other three algorithms. For example, the average cost of IMOGA-TS is \$6511, while the cost of MOGA, NSGA-II, and MOHSA are \$7,094, \$6,958, and \$7,077, respectively. Second, the minimum average number of vehicles (i.e., 22 vehicles) are obtained in the IMOGA-TS optimization results, thus saving 4, 2, and 3 compared with MOGA, NSGA-II, and MOHSA respectively. Third, the IMOGA-TS outperforms NSGA-II, MOGA, and MOHSA in terms of the number of used CSs and the minimum computation time. To further test the performance of the proposed IMOGA-TS algorithm, various validation indicators, including hyper-volume (HV), number of Pareto solution (NOP), and mean ideal distance (MID) are used to evaluate both diversity and convergence of the Pareto-optimal front (Wei et al., 2020; Zarouk, Mahdavi, Rezaeian, & Santos-Arteaga, 2022). The computational results of Instances 1–20 with the three indicators among four algorithms are shown in Table 11. In addition, the average values of the three validation indicators among four algorithms are shown in Table 12.

In Table 12, three validation indicators (i.e., HV, NOP, and MIP) are utilized to evaluate the Pareto-optimal front obtained by the four metaheuristics. The non-dominated solutions can be obtained by the proposed IMOGA-TS with the highest average HV and NOP, which means non-dominated solutions from the proposed algorithm have a better spread performance and are closer to the Pareto-optimal front. The average MID value of IMOGA-TS is lower than those of other three algorithms, indicating the proposed IMOGA-TS outperforms the other three solution algorithms in finding a more uniformly distributed Pareto front and having better convergence performance. Therefore, the comparison result indicates that the proposed IMOGA-TS is superior to the other three algorithms in solving CMEVRPTW-SCS.

6.2. Data description

To verify the practical significance and effectiveness of the proposed model and algorithm, a real case study in Chongqing City, China is adopted. This logistics network has four depots (i.e., D1, D2, D3, D4), 13 CSs (i.e., CS1, CS2,..., CS13), and 143 customers (i.e., C1, C2,..., C143). The demands of these customers will be served by different depots, and each depot has its own electric fleet and CSs. Fig. 11 presents the spatial distribution of depots, CSs, and customers for the logistics network, and the initial characteristics of the logistics facilities are described in Table 13. With the popularity of EVs, the charging resources become

¹ <https://neo.lcc.uma.es/vrp/vrp-instances/multiple-depot-vrp-instances/>.

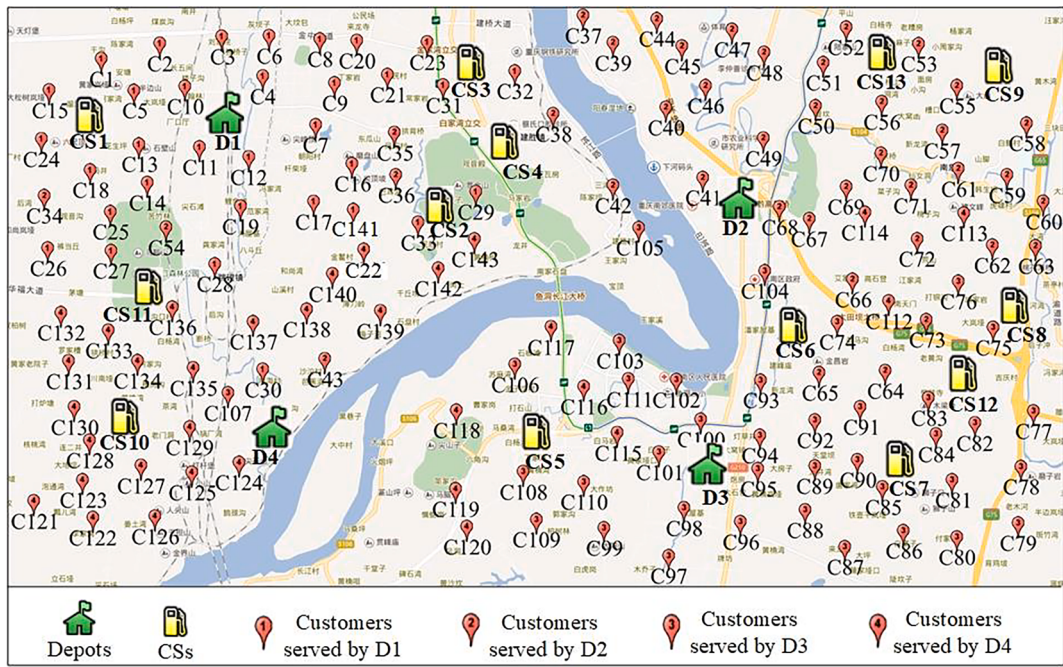


Fig. 11. Spatial distribution of logistics facilities and customers.

more and more scarce, which makes the CSs belonging to the depot have a long-distance distribution as shown in Fig. 11. On the basis of the related references (Kancharla & Ramadurai, 2020; Basso et al., 2021; Wang, Peng, & Xu, 2021), actual surveys, and stability analysis of parameter selection, the parameters used in the model formulation are

Table 14
Parameter settings.

Parameter	Description	Value
δ_v	Arc specific coefficient of EV $v, v \in V$	0.11
ℓ_t	Arc specific coefficient of EV $v, t \in TR$	0.13
β_v	Vehicle specific coefficient of EV $v, v \in V$	0.76
τ_t	Vehicle specific coefficient of ET $t, t \in TR$	0.79
FV_v	Rental cost of EV $v, v \in V$	100
FT_t	Rental cost of ET $t, t \in TR$	180
F_d	Fixed cost of depot $d, d \in D$	200
μ_d	Variable cost coefficient of depot $d, d \in D$	0.5
f_e	Electricity price, (unit: \$)	2.5
f_{ch}	Charging cost of electricity per unit time, (unit: \$/h)	5
wv_v	Weight of EV $v, v \in V$ (unit: kg)	2000
wt_t	Weight of ET $t, t \in TR$ (unit: kg)	4000
a_v	Acceleration of EV $v, v \in V$, (unit: m/s ²)	0
g	Gravitational constant, (unit: m/s ²)	9.81
θ	Road inclination angle	0
λ_v	Rolling friction coefficient of EV $v, v \in V$	0.01
σ	Air drag coefficient	0.48
A_v	Frontal area of EV $v, v \in V$ (unit: m ²)	2.3301
ρ	Air density, (unit: kg/m ³)	1.2041
ζ_v	Drive train efficiency of EV $v, v \in V$	0.89
SV_v	Speed of EV $v, v \in V$ (unit: m/s)	11.12
ST_t	Speed of ET $t, t \in TR$ (unit: m/s)	11.12
δ_v	Charging rate of EV $v, v \in V$, (unit: kWh/h)	30
PE_e	Penalty cost per unit of time of earliness	5
PD_l	Penalty cost per unit of time of delay	10
E_v	Battery capacity of EV $v, v \in V$, (unit: kWh)	60
SOC_{min}	State of charge of EV $v, v \in V$	25 %
l_{max}	Maximum travel distance of EV $v, v \in V$ (unit: km)	100
Q_v	Load capacity of EV $v, v \in V$, (unit: kg)	200
U_t	Load capacity of ET $t, t \in TR$, (unit: kg)	1500
$popsize$	Population size	100
ps	Selection probability	0.8
pc	Crossover probability	0.8
pm	Mutation probability	0.2

set in Table 14. The stability of heuristic algorithm is significantly investigated by the sensitivity of parameters in the process of searching optimal solutions (Long et al., 2019; Wang, Li, Guan, Xu, et al., 2021; Wang, Zhe, et al., 2022). Furthermore, a stability analysis is performed to obtain appropriate parameters of the proposed IMOOGA-TS. In the sensitivity analysis, the total operating cost (TOC) and standard deviation (SD) are calculated by running the proposed algorithm 20 times with the adjustment of the key parameters, including the selection probability (ps), crossover probability (pc), and mutation probability (pm). Table 15 exhibits the computation results of 20 scenarios. The TOC and SD are fluctuated with the tuning of parameters. The most appropriate set of the three key parameters with the smallest TOC and SD are selected to improve the stability and efficiency of the IMOOGA-TS. Therefore, the lowest TOC (i.e., \$6476) and SD (i.e., 3) can be achieved when ps is determined as 0.8. Similarly, pc can be set as 0.8 with the lowest TOC (i.e., \$6476) and SD (i.e., 5), and pm can be determined as 0.2 with the lowest TOC (i.e., \$6476) and SD (i.e., 2).

6.3. Optimization results

6.3.1. Clustering results

To simplify the calculation difficulty of CMEVRPTW-SCS, GMCA is used to cluster the customers on the basis of two dimensions: time and space. The specific clustering results are shown in Fig. 12, where X represents the longitude, Y denotes the latitude, and Z indicates the time. In addition, Table 16 shows the update of customer service relationships because of the customer clustering.

In Fig. 12, 143 customers are reassigned to the corresponding four depots. To be specific, 34 customers are assigned to D1, 42 customers are assigned to D2, 40 customers are assigned to D3, and 27 customers are assigned to D4. From the perspective of time clustering, customers are distributed along the Z -axis, which can facilitate the EVs' delivery to satisfy customers' service time windows. From the perspective of the spatial clustering results, customers are distributed around each depot, which is beneficial to shorten the delivery distance and save costs. The reallocation of customer service has changed the affiliation between customers and depots. In Table 16, the service relationship of 22 customers has been changed, thus leading to the service customers' increase

Table 15

Computation result comparison among different values of parameters.

Scenario	<i>ps</i>	-			<i>pc</i>	-			<i>pm</i>	-		
	Value	TOC (\$)	SD	-	Value	TOC (\$)	SD	-	Value	TOC (\$)	SD	-
1	0.05	6593	16	-	0.3	6707	25	-	0.01	6519	10	-
2	0.1	6587	15	-	0.4	6699	23	-	0.05	6498	9	-
3	0.15	6571	12	-	0.45	6688	20	-	0.15	6494	5	-
4	0.2	6552	14	-	0.47	6686	18	-	0.2	6476	2	-
5	0.25	6548	13	-	0.5	6676	18	-	0.25	6476	3	-
6	0.3	6545	11	-	0.55	6672	15	-	0.3	6545	4	-
7	0.35	6531	10	-	0.57	6669	13	-	0.35	6561	6	-
8	0.4	6512	9	-	0.6	6663	10	-	0.4	6593	7	-
9	0.45	6501	9	-	0.65	6536	9	-	0.45	6597	9	-
10	0.5	6500	8	-	0.67	6522	9	-	0.5	6625	9	-
11	0.55	6495	8	-	0.7	6511	8	-	0.55	6653	10	-
12	0.6	6493	7	-	0.75	6510	6	-	0.6	6658	11	-
13	0.65	6489	6	-	0.77	6504	5	-	0.65	6673	11	-
14	0.7	6484	5	-	0.8	6476	5	-	0.7	6678	13	-
15	0.75	6477	5	-	0.85	6476	6	-	0.75	6749	15	-
16	0.8	6476	3	-	0.87	6564	9	-	0.8	6766	16	-
17	0.85	6476	6	-	0.9	6586	9	-	0.85	6770	17	-
18	0.9	6564	9	-	0.95	6593	11	-	0.9	6771	20	-
19	0.95	6623	11	-	0.97	6607	13	-	0.95	6774	20	-
20	1	6687	13	-	1	6662	14	-	1	6803	22	-

or decrease for each depot. For example, the number of D2's service customers have been increased by eight; the facility assignment of C30 is changed from D1 to D4 after customer clustering.

6.3.2. Vehicle routing optimization with shared charging stations

The introduction of collaboration mechanisms in CMEVRPTW-SCS promotes the sharing of customer services among multiple depots. Each customer is reassigned to the shortest depot through GMCA, which minimizes the delivery cost. Moreover, the adoption of the CS sharing strategy in CMEVRPTW-SCS greatly improves resource utilization. The increase in the EV loading rate contributes to the reduction of the number of EVs. Therefore, the logistics network is reconstructed and the optimization results are obtained through the proposed CMEVRPTW-SCS optimization. The specific optimization results, including facility operating cost (FOC), centralized transportation cost (CTC), electric delivery cost (EDC), penalty cost (PC), charging cost (CC), total operating cost (TOC), and electricity consumption (EC) are shown in Table 17 and Fig. 13. The initial results are calculated by the non-optimized routes from the data survey of the real-world EV

distribution network, and the optimized results are computed by the proposed solution methods.

The total cost, the number of used EVs, and the electricity consumption of each depot in the optimized logistics network can be reduced through the optimization procedure of initial delivery routes based on the proposed solution methods. In Table 17 and Fig. 13, the violation of time windows has been alleviated after optimization, and the penalty cost has decreased from \$470 to \$155. The total cost has decreased from the initial \$12,047 to \$6,476, with a reduced rate of 46.2 %. The number of EVs has decreased from 29 to 13, with a drop of

Table 16
Service relationship characteristics of customers.

Depots	Customers with changed service relationships	Number of customers
D1	C34 C35 C36 C54 C141	5
D2	C32 C74 C75 C76 C105 C112 C113 C114	8
D3	C64 C65 C115 C116 C117 C118 C119 C120	8
D4	C30 C43 C22	3

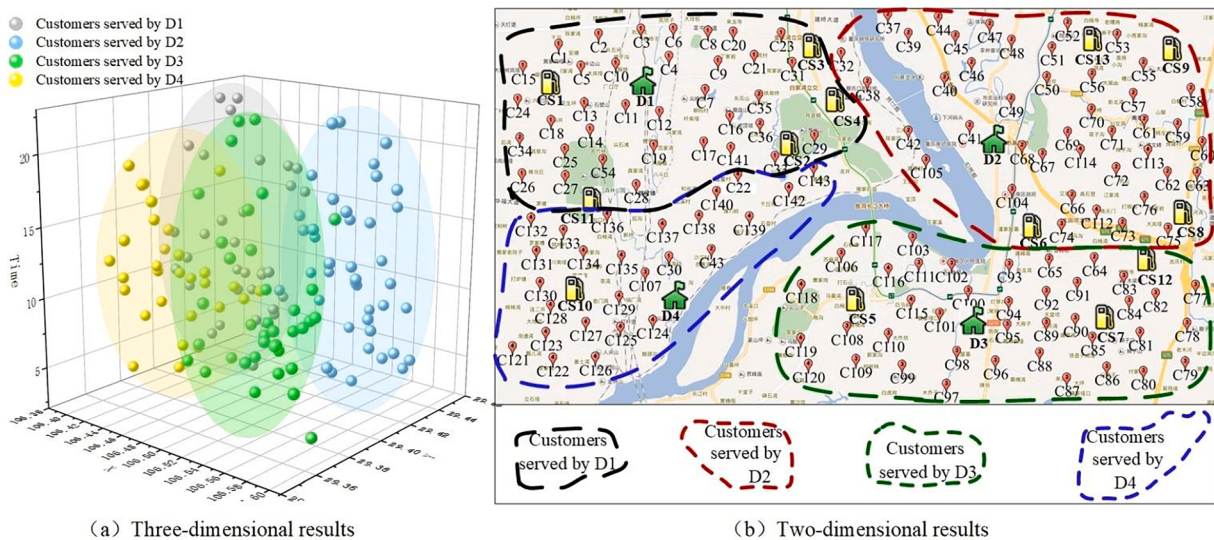


Fig. 12. Gaussian mixture clustering results in CMEVRPTW-SCS.

Table 17

Comparison of the results before and after optimization.

Case	Depots	FOC (\$)	CTC (\$)	EDC (\$)	CC (\$)	PC (\$)	TOC (\$)	EC (kWh)	Number of customers	Number of EVs	Number of ETs	Number of used CSs	Number of shared CSs
Initial	D1	200	0	2349	93	84	2726	940	33	6	0	5	0
	D2	200	0	2870	149	186	3405	1148	40	8	0	4	0
	D3	200	0	2655	84	103	3042	1062	37	7	0	3	0
	D4	200	0	2486	91	97	2874	994	32	8	0	1	0
	Total	800	0	10,360	417	470	12,047	4144	142	29	0	13	0
Optimized	D1	269	284	793	114	31	1491	317	34	3	1	4	2
	D2	295	396	920	181	58	1850	368	42	4	1	3	1
	D3	258	347	828	137	32	1602	331	40	3	1	2	1
	D4	237	309	831	122	34	1533	332	27	3	1	2	1
	Total	1059	1336	3372	534	155	6476	1348	142	13	4	10	5

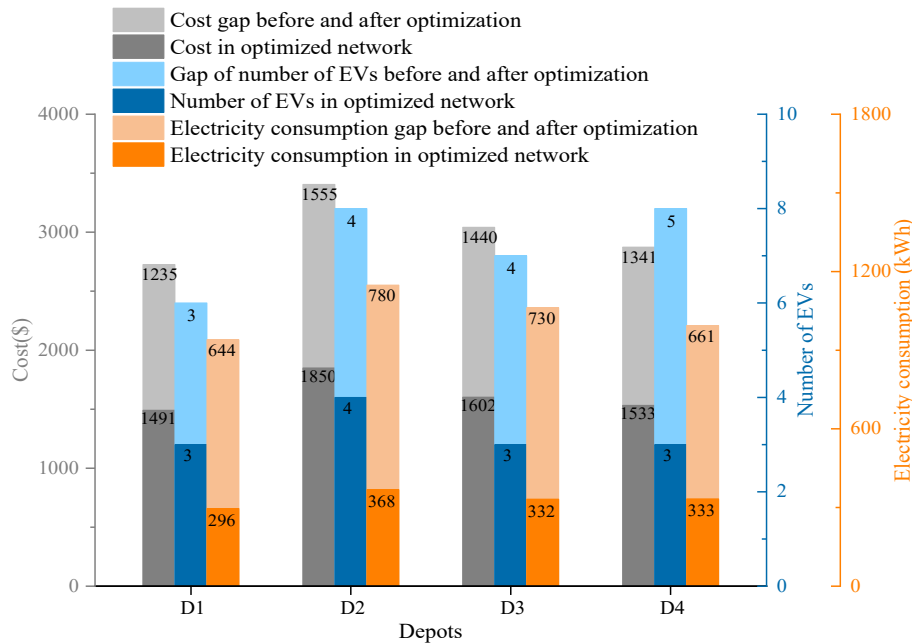


Fig. 13. Comparison of the results before and after optimization.

55 %. The electricity consumption of EVs has decreased from 4144 to 1348 kWh, thus achieving a decrement of 67 %. Moreover, the number of used CSs has decreased by 3 as a result of the implementation of the CS sharing strategy. The comparison results intuitively show the gap before and after the optimization of total operating costs, electricity

consumption and number of EVs. The specific optimized EV routes are shown in Table 18 and Fig. 14.

In Table 18 and Fig. 14, the total number of delivery routes is 13, thus denoting that 16 routes have been reduced compared with the initial distribution network. In the optimized logistics network, the

Table 18

Optimal routes in CMEVRPTW-SCS.

Depots	EVs	Optimal distribution routes
D1	EV1	C10 → C5 → C2 → C1 → C15 → C24 → CS1 → C13 → C18 → C34 → C14 → C11
	EV2	C4 → C3 → C6 → C8 → C20 → C23 → CS3* → C31 → C21 → C9
	EV3	C12 → C19 → C25 → C26 → C27 → CS11* → C54 → C17 → C22 → C33 → CS2* → C29 → C36 → C16 → C35 → C7
D2	EV4	C46 → C47 → C45 → C44 → C39 → C37 → CS3* → C32 → C38 → C40
	EV5	C69 → C71 → C61 → C59 → C60 → C63 → C62 → C75 → CS12* → C76 → C72 → C113 → C114
	EV6	C49 → C50 → C48 → C51 → C52 → C53 → CS9 → C55 → C58 → C57 → C56 → C70
D3	EV7	C68 → C67 → C66 → C112 → C73 → C74 → CS6* → C104 → C105 → C42 → C41
	EV8	C115 → C116 → C111 → C103 → C117 → C106 → C118 → CS5 → C110 → C108 → C119 → C120 → C109 → C99 → C97 → C98
	EV9	C96 → C88 → C87 → C86 → C80 → C79 → C78 → C81 → CS7 → C85 → C90 → C89 → C95
D4	EV10	C100 → C102 → C93 → C65 → CS6* → C64 → C83 → C82 → C77 → CS12* → C84 → C91 → C92 → C94
	EV11	C107 → C125 → C127 → C122 → C126 → C124
	EV12	C135 → C134 → C136 → CS11* → C133 → C132 → C131 → C130 → CS10 → C128 → C121 → C123 → C129
	EV13	C30 → C138 → C137 → C28 → C140 → C141 → CS2* → C143 → C142 → C139 → C43

CS: used charging stations.

CS*: shared charging stations.

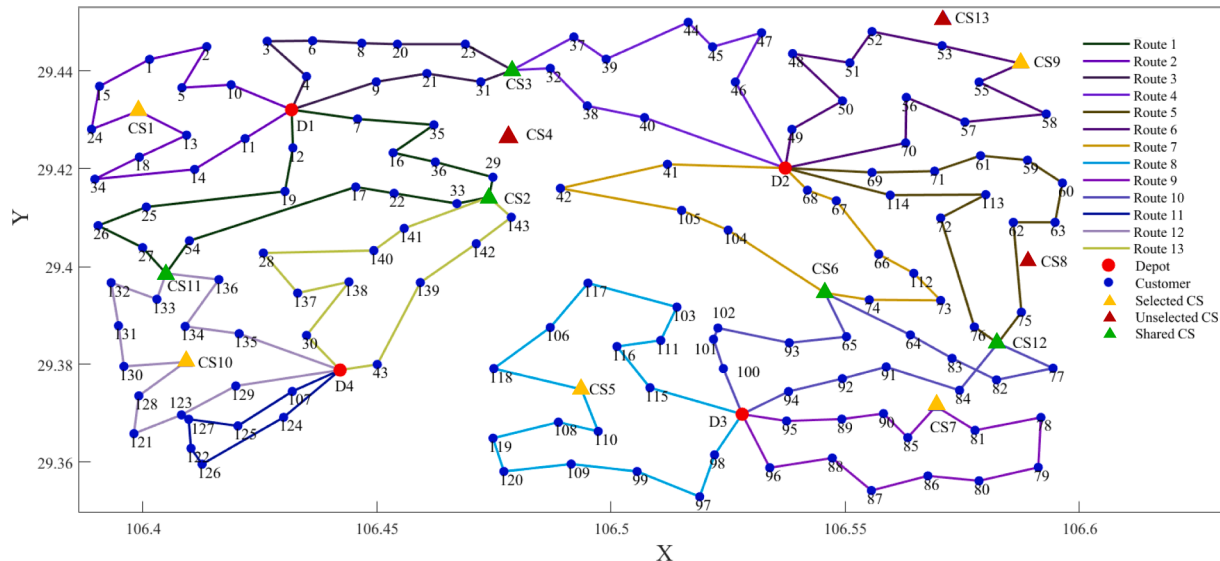


Fig. 14. Optimized EV routes of four depots in CMEVRPTW-SCS.

increase in the number of service customers on each delivery route can greatly improve the loading rate of EVs and reduce the total delivery distance. Moreover, by enabling charging station sharing, ten CSs are used to provide charging services for EVs in 13 delivery routes, thus saving three CSs in total. Additionally, five CSs are shared among different depots and EVs. To be specific, CS3 is shared between D1 and D2; CS11 and CS2 are shared between D1 and D4; CS6 and CS12 are shared between D2 and D3. Therefore, the sharing of CSs and the optimization of delivery routes can reduce the number of required EVs and total operating cost to realize the resource saving of the whole transportation system.

6.3.3. Profit allocation results

The CMEVRPTW-SCS optimization seeks a routing solution with the lowest total operating cost and the lowest number of EVs through the collaborative mechanism and CS sharing strategy. If all depots agree to collaborate, 2^4-1 alliance scenarios will be available, excluding the null one. Table 19 and Fig. 15 summarize the comparison results before and after the optimization of each alliance in terms of the total operating cost (Cost), number of EVs (EVs), number of used CSs (Used CSs), and number of shared CSs (Shared CSs). The initial results of single depot alliance are achieved by calculation based on the initial delivery routes obtained from the investigation, and the optimized ones is realized by

simultaneously optimizing the EV distribution routes and implementing the CS sharing strategy. In addition, the results of multidepot alliance are computed by the proposed IMOGA-TS.

In Table 19, compared with the initial network, the total operating cost, the number of EVs, the electricity consumption, and the number of used CSs have all been reduced, and the number of shared CSs has increased. This phenomenon demonstrates that the collaborative mechanism has a positive impact on cost reduction and resource utilization improvement. In Fig. 15, the gap between the initial network and the optimized network is more intuitive. With the increase of the number of alliance members, cost savings, electricity savings and CS savings all show an increasing trend. The redistribution of customer service and the sharing of CSs in the optimized collaborative network allow EVs to serve customers more flexibly, thereby reducing the driving distance and the number of used CSs. Collaborative mechanism induces additional profits, thus arousing the interest of alliance participants in profit distribution. Driven by interests, depots gradually join the collaboration alliance, which leads to the reduction of the total operating cost of the whole logistics network. Moreover, the reduced cost becomes the additional profit allocated to alliance members.

The allocated benefits of the alliance come from the cost savings generated by the sharing of customer service and CSs among multiple depots. The demands of customers are satisfied by their corresponding

Table 19

Comparison of different alliances.

Alliances	Initial					Optimized				Gap				
	Cost (\$)	EVs	EC (kWh)	Used CSs	Shared CSs	Cost (\$)	EVs	EC (kWh)	Used CSs	Shared CSs	Cost (\$)	EVs	EC (kWh)	Used CSs
{D1}	2726	7	940	4	0	2091	5	577	4	1	635	2	363	0
{D2}	3405	8	1148	4	0	2729	6	723	4	0	676	2	425	0
{D3}	3042	7	1062	3	0	2399	5	659	3	1	643	2	403	0
{D4}	2874	7	994	1	0	2228	4	561	2	0	646	3	433	1
{D1, D2}	4420	16	1676	8	0	2815	13	1007	7	1	1605	3	669	1
{D1, D3}	4290	15	1553	7	0	2646	13	928	6	1	1644	2	625	1
{D1, D4}	3819	15	1420	6	0	2274	12	787	5	1	1545	3	633	1
{D2, D3}	4728	16	1767	7	0	2888	13	1069	6	2	1840	3	698	1
{D2, D4}	4757	15	1624	6	0	2980	13	1005	5	1	1777	2	619	1
{D3, D4}	4627	15	1514	5	0	2789	13	896	4	1	1838	2	618	1
{D1, D2, D3}	8419	24	2306	11	0	4577	17	1264	9	2	3842	7	1042	2
{D1, D2, D4}	8248	23	2198	10	0	4420	17	1152	8	3	3828	6	1046	2
{D1, D3, D4}	8003	23	2115	9	0	4371	18	1103	7	2	3632	5	1012	2
{D2, D3, D4}	9056	24	2471	9	0	4769	17	1424	7	3	4287	8	1047	2
{D1, D2, D3, D4}	12,047	29	4144	13	0	6476	13	1348	10	5	5571	16	2796	3

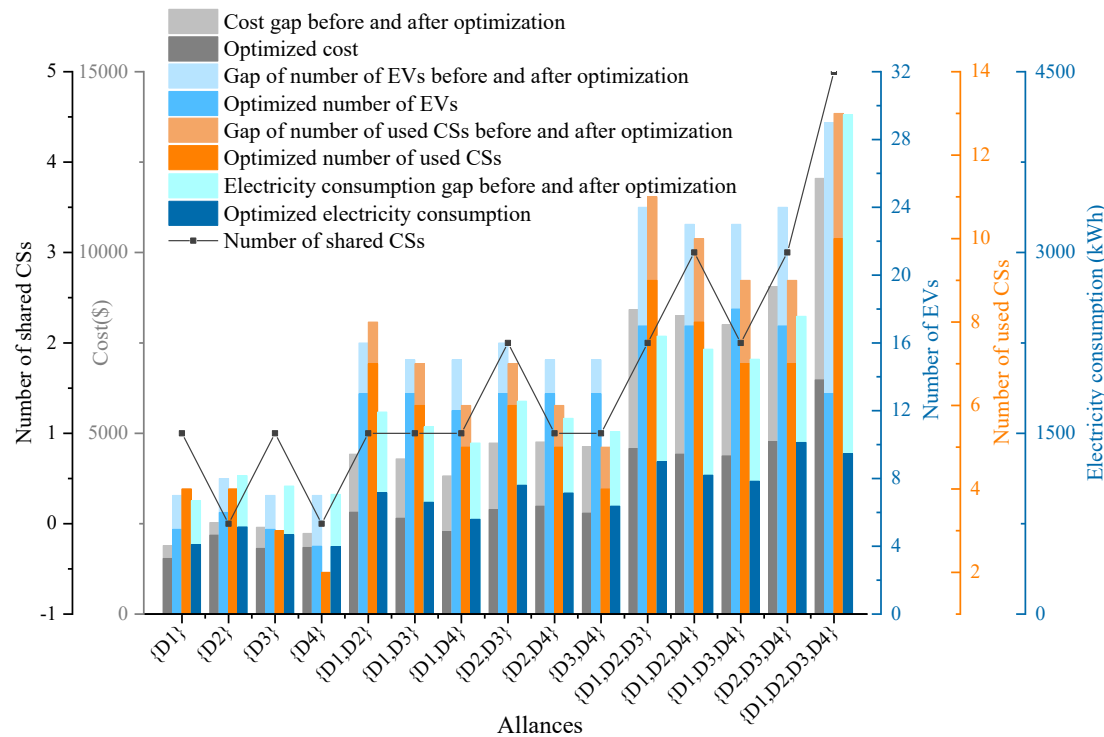


Fig. 15. Results between initial and optimized network in different alliances.

depots, and the EVs provide delivery services to customers come from depots, and the CSs belong to multiple depots. Therefore, the benefits are allocated among the depots participating in the alliance. Table 20 shows the profit allocation to each participant as the alliance is formed on the basis of the Shapley value model.

In Table 20, the results show that an individual with more cost savings will obtain the higher profit allocation in the alliance, because the greater contribution can be made for the alliance. For example, D1 with a cost saving of \$635 is less than D3 with \$653, and they can achieve \$793 and \$851 in alliance {D1, D3}, respectively. The amount of profit available for each depot increases as the alliance deepens, and the participant gains most when the grand alliance is formed. For example, when four depots operate independently, they can obtain \$635, \$676, \$653, and \$646, respectively. However, in the grand

Table 20
Profit allocation for each member in the collaborative alliance.

Alliances	Initial cost	Optimized cost	Cost saving	Profit allocation			
				D1	D2	D3	D4
{D1}	2726	2091	635	635	0	0	0
{D2}	3405	2729	676	0	676	0	0
{D3}	3042	2389	653	0	0	653	0
{D4}	2874	2228	646	0	0	0	646
{D1, D2}	4420	2815	1605	799	806	0	0
{D1, D3}	4290	2646	1644	793	0	851	0
{D1, D4}	3819	2274	1545	741	0	0	804
{D2, D3}	4728	2888	1840	0	950	890	0
{D2, D4}	4757	2980	1777	0	940	0	837
{D3, D4}	4627	2789	1838	0	0	920	918
{D1, D2, D3}	8419	4577	3842	1130	1328	1184	0
{D1, D2, D4}	8248	4420	3828	1188	1354	0	1286
{D1, D3, D4}	8003	4371	3632	1103	0	1303	1226
{D2, D3, D4}	9056	4769	4287	0	1449	1432	1406
{D1, D2, D3, D4}	12,047	6476	5571	1123	1571	1454	1423

Table 21
Profit allocation according to EPM, MCRS, Shapley, and GQP.

Method	Profit allocation	Core center	Distance
EPM	(1240,1539,1411,1381)	(1078,1613,1450,1429)	349
MCRS	(1203,1491,1454,1423)		175
Shapley	(1123,1571,1454,1423)		62
GQP	(1240,1539,1411,1381)		90

alliance, their profits increase to \$1123, \$1571, \$1454 and \$1423, respectively. To verify the effectiveness of the Shapley value model, three methods, including the minimum cost remaining savings model (MCRS), the cost gap allocation model (CGA), and the equal profit method (EPM) model are adopted to calculate the allocation results. Then, the results of each profit allocation mechanism are compared on the basis of the distance to the core center to determine the performance of each method. Based on the snowball theory (Comi, Schiraldi, &

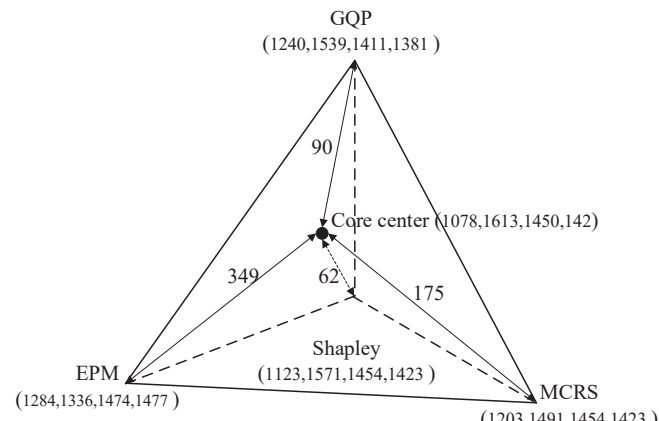


Fig. 16. Core center and distance comparison diagram.

Table 22

Optimization result comparison based on three scenarios.

Case	FOC (\$)	CTC (\$)	EDC (\$)	CC (\$)	PC (\$)	TOC (\$)	EC (kWh)	Number of EVs	Number of ETs	Number of used CSs	Number of shared CSs
Noncollaboration	800	0	8385	393	392	9970	3354	21	0	13	0
Collaboration without CS sharing	1059	1336	5050	378	206	8029	2020	16	4	12	0
Collaboration with CS sharing	1059	1336	3392	534	155	6476	1348	13	4	10	5

Buttarazzi, 2018; Feng, Pang, Lodewijks, & Li, 2017), the closer to the core is, the better the method becomes. Therefore, the position of the core center must be determined. Eq. (48) shows the formula of calculating the core center.

$$v(N - \{n\}) = \frac{v(N) - v(N - \{n\})}{v(N)} \times \delta + \sum_{i \in N}^{n \neq i} y_i \quad (48)$$

where $v(N)$ is the total cost savings of the grand alliance N , n represents an alliance member, and δ is a parameter for controlling the scope of the core. y_i represents the core center of each participant n in the grand alliance. The four different profit allocation results for each depot are shown in Table 21 and Fig. 16.

In Table 21 and Fig. 16, the numbers in parentheses represent the profit allocation results for D1, D2, D3, and D4, respectively. The distance calculated by the Shapley value model is the closest to the core center. The result shows the superiority of the model in this case compared with the other three profit allocation methods. Therefore, the Shapley value model is the most appropriate profit allocation method.

6.4. Analysis and discussion

6.4.1. Comparison of various collaboration mechanisms

The collaboration mechanism and the CS sharing strategy greatly influence the proposed CMEVRPTW-SCS optimization. To verify the superiority of the collaboration mechanism, three scenarios, including noncollaboration, collaboration without CS sharing, and collaboration with CS sharing, are considered on the basis of the studied logistics network. Then, the CS sharing strategy is introduced into collaborative optimization to discuss the impact on the optimization of CMEVRPTW-SCS further. Table 22 and Fig. 17 analyze and discuss the influence of

collaboration on CMEVRPTW-SCS optimization by comparing the three scenarios. The comparative indicators are facility operating cost (FOC), centralized transportation cost (CTC), electric delivery cost (EDC), penalty cost (PC), charging cost (CC), total operating cost (TOC), electricity consumption (EC), and numbers of EVs, ETs, CSs, and shared CSs.

In Table 22 and Fig. 17, a comparison of the collaborative and noncollaborative optimized networks shows that the total cost is decreased from \$9,970 to \$8,029, achieving a 20 % cost-reduction. The number of EVs changes from 21 to 16, with seven reductions for delivery routes, and the number of used CSs is decreased from 13 to 12. The electricity consumption of EVs is reduced from 3354 to 2020 kWh, thus, obtaining 40 % energy savings. Therefore, the collaborative optimization of CMEVRPTW-SCS can maximize the utilization of vehicles, CSs, and electricity resource. In addition, the total operating cost decreases from \$8,529 to \$6,476, the number of EVs decreases from 16 to 13, and the electricity consumption reduces from 2,020 to 1,348 kWh. The reduction in cost energy and number of required EVs demonstrates the effectiveness of the CS sharing strategy. Moreover, compared with the mode without CS sharing, the number of used CSs when adopting CS sharing is saved by 2, thus realizing great improvement in resource utilization. Table 23 and Fig. 18 show the electric delivery routes, total operating cost (Cost), number of EVs, and electricity consumption (EC) of D2 and D3 in three scenarios.

In Table 23 and Fig. 18, the EV routes of three scenarios are presented. In the noncollaboration network, the facilities do not work with one another, thus resulting in long-distance transportation and inefficient transportation. In the logistics network of collaboration without CS sharing, the construction of a collaborative mechanism has eliminated long-distance transportation and reduced the total operating cost. Meanwhile, the transport inefficiency remains unsolved. For example, the EV merely serves six customers before returning to D3. In the

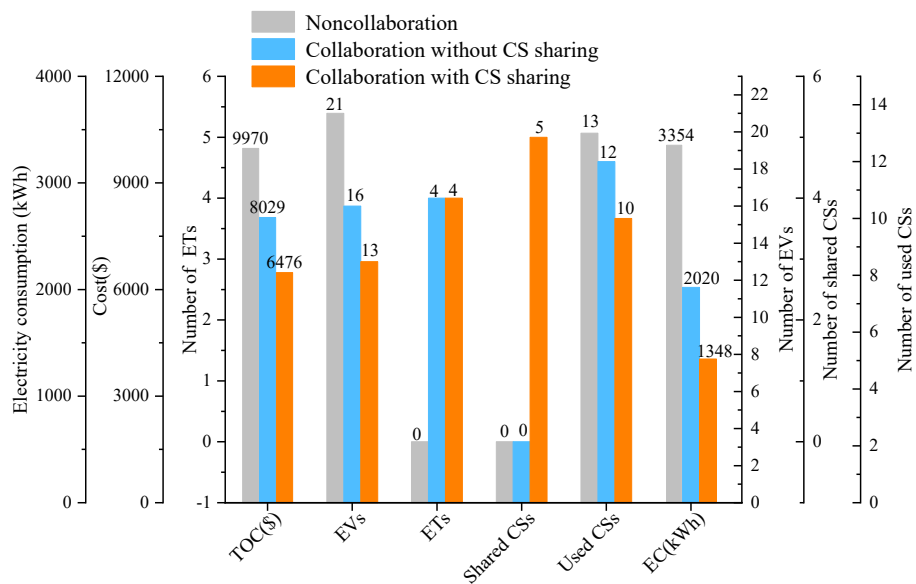


Fig. 17. Optimization result comparison based on three scenarios.

Table 23

Electric delivery routes of D3 in three scenarios.

Scenarios	Depots	Routes	Total Cost (\$)	Cost (\$)	Number of EVs	EC (kWh)	Total EC (kWh)
Non-collaboration	D2	C43 → C54 → C34 → C35 → C36 C46 → C45 → C44 → C37 → C39 → C38 → C40 C68 → C66 → C64 → C65 → C56 → C41 → C42 C72 → C62 → C59 → C60 → C63 → C58 → C73 → C67 C70 → C57 → C53 → C59 → C58 → C61 → C71 → C69 C49 → C48 → C47 → C51 → C52 → C53 → C55 → C56 → C50	5896	3155	6	965	1839
	D3	C103 → C105 → C104 → C102 → C100 C95 → C89 → C90 → C94 C74 → C76 → C75 → C77 → C82 → C57* → C84 → C83 → C91 → C92 C98 → C97 → C99 → C109 → C110 → C108 → C55 → C107 → C106 → C111 → C101 → C93 C96 → C87 → C86 → C80 → C79 → C78 → C57* → C81 → C82 → C88	2741	2741	5	874	874
Collaboration without CS sharing	D2	C40 → C38 → C32 → C37 → C39 C70 → C57 → C38 → C55 → C59 → C53 → C56 → C50 C46 → C45 → C44 → C47 → C52 → C53 → C51 → C48 → C49 C68 → C67 → C66 → C74 → C56 → C104 → C105 → C42 → C41 C69 → C71 → C61 → C59 → C60 → C62 → C63 → C58 → C75 → C76 → C73 → C72 → C113 → C114	4464	2396	5	608	1171
	D3	C115 → C116 → C117 → C103 → C100 C93 → C102 → C111 → C106 → C118 → C55 → C110 → C108 → C119 → C120 → C109 → C99 → C97 → C98 C96 → C88 → C87 → C86 → C80 → C79 → C78 → C81 → C57 → C85 → C90 → C89 → C95 C65 → C64 → C83 → C77 → C512* → C82 → C84 → C91 → C92 → C94 C46 → C47 → C45 → C44 → C39 → C37 → C53* → C32 → C38 → C40 C69 → C71 → C61 → C59 → C60 → C63 → C62 → C75 → C512* → C76 → C72 → C113 → C114 C49 → C50 → C48 → C51 → C52 → C53 → C59 → C55 → C58 → C57 → C56 → C70 C68 → C67 → C66 → C112 → C73 → C74 → C56* → C104 → C105 → C42 → C41	2095	2095	4	563	563
Collaboration with CS sharing	D2	C115 → C116 → C117 → C103 → C100 → C118 → C55 → C110 → C108 → C119 → C120 → C109 → C99 → C97 → C98 C96 → C88 → C87 → C86 → C80 → C79 → C78 → C81 → C57 → C85 → C90 → C89 → C95 C100 → C102 → C93 → C65 → C56* → C64 → C83 → C82 → C77 → C512* → C84 → C91 → C92 → C94	3452	1850	4	368	699
	D3	C115 → C116 → C111 → C103 → C117 → C106 → C118 → C55 → C110 → C108 → C119 → C120 → C109 → C99 → C97 → C98 C96 → C88 → C87 → C86 → C80 → C79 → C78 → C81 → C57 → C85 → C90 → C89 → C95	1602	1602	3	331	331

CS: used charging stations.

CS*: shared charging stations.

logistics network of collaboration with CS sharing, the number of customers served by one vehicle can reach to 12, thus obtaining a significant improvement. In addition, the collaboration mechanism and the CS sharing strategy have contributed to savings in cost, number of EVs, and electricity consumption. For example, the total operating cost of D2 and D3 is reduced from \$5,896 in the noncollaboration network to \$4,464 in the network of collaboration without CS sharing, and thus finally achieving the minimum cost of \$3,452 in the logistics network of collaboration with CS sharing. Therefore, the collaborative mechanism and the CS sharing strategy are both beneficial to improve transportation efficiency and reduce operating costs.

6.4.2. Comparison of various alliances with or without shared CSs

The implementation of the CS sharing strategy and the scale of the cooperative alliance can affect the optimization degree of the collaborative logistics network. Its superiority can be further verified by the total cost, number of EVs, and other economic indicators. In this section, the logistics networks with and without shared CSs under the collaboration framework are compared to analyze and discuss the influence of the CS sharing strategy in different alliances on CMEVRPTW-SCS optimization. The specific comparison results, including total operating cost (TOC), number of EVs (EVs), number of used CSs (used CSs), number of shared CSs (shared CSs), and electricity consumption (EC) are shown in Table 24 and Fig. 19.

In Table 24 and Fig. 19, the total operating cost, the number of EVs, the number of used CSs and the electricity consumption of EVs show a

significant downward trend with the implementation of the CS sharing strategy. Moreover, the reduction of the total cost, number of EVs, number of used CSs, and electricity consumption grows with the expansion of the alliance. The phenomenon justifies the superiority of the coalition in CMEVRPTW-SCS. The more CSs are shared, the costs are lower, and the fewer EVs are required when the scale of alliance is the same, thus reflecting the effectiveness of the CS sharing strategy. For example, alliance {D1, D2, D3}, D4 shares one more CS than alliance (D1, {D2, D3, D4}). Meanwhile, the cost decreases from \$7,051 to \$6,897 and the number of required EVs decreases from 21 to 18. Table 25 and Fig. 20 show the electric delivery routes, total operating cost (Cost), number of EVs, and electricity consumption (EC) of D1 and D4 in the optimized network without and with shared CSs.

In Table 25 and Fig. 20, the number of required EVs of D1 and D4 have been reduced from four to three in the collaborative networks when considering CS sharing among multiple depots. In Fig. 18(a), eight EV routes are available for 62 customers in the optimized network without shared CSs. In Fig. 18(b), the CS sharing strategy is introduced in the optimized network to reduce the total operating cost and improve transportation efficiency. The customers served by each EV increase on the basis of the CS sharing. The maximum number of customers served by an EV can reach up to 14. Thus, the transportation efficiency is greatly improved. Moreover, the total cost, the number of EVs, and the electricity consumption of D1 and D4 decrease from \$4056, 8, and 912 kWh to \$3093, 6, and 649 kWh, respectively, after the implementation of the CS sharing strategy. Therefore, the CS sharing strategy proposed

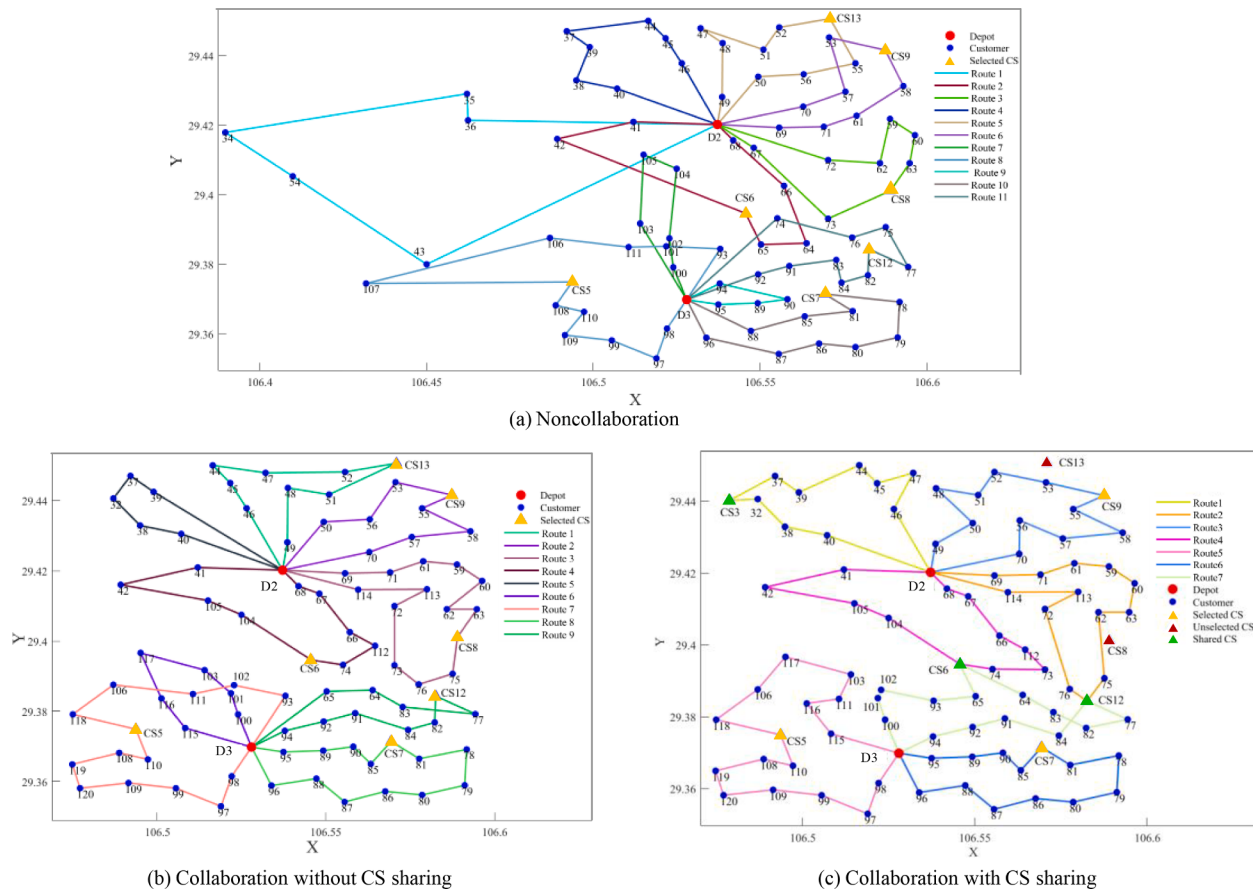


Fig. 18. EV routes comparison in three scenarios.

in this study can promote the optimization of EV routes and the improvement of transportation efficiency in the CMEVRPTW-SCS.

6.5. Management insights

In this study, the collaborative mechanism and the CS sharing

strategy are effectively applied to coordinate the delivery routes of EVs in a multidepot logistics network. The management insights of this study can be summarized as follows:

(1) The collaborative mechanism and CS sharing strategy are beneficial to generate economic and ecological profits, and promote the operational efficiency of logistics networks in the CMEVRPTW-SCS.

Table 24
Optimization result comparison of various alliances.

Alliances	Without shared CSs					With shared CSs					Gap			
	Cost (\$)	EVs	Used CSs	Shared CSs	EC (kWh)	Cost (\$)	EVs	Used CSs	Shared CSs	EC (kWh)	Cost (\$)	EVs	Used CSs	EC (kWh)
{(D1, D2), D3, D4}	8663	21	13	0	1946	7139	19	12	2	1670	1524	2	1	276
{(D1, D3), D2, D4}	8735	22	13	0	1905	7153	20	12	2	1628	1582	2	1	277
{(D1, D4), D2, D3}	8792	21	13	0	1770	7265	19	12	2	1486	1527	2	1	284
(D1, {D2, D3}, D4)	8747	22	13	0	2000	7412	20	12	2	1718	1335	2	1	282
(D1, {D2, D4}, D3)	8839	22	13	0	1927	7241	20	12	1	1653	1598	2	1	274
(D1, D2, {D3, D4})	9028	23	13	0	1811	7544	21	12	1	1581	1484	2	1	230
{(D1, D2, D3), D4}	8554	21	13	0	2025	6897	18	11	4	1596	1657	3	2	429
{(D1, D3, D4), D2}	8607	21	13	0	1886	6933	18	11	4	1483	1674	3	2	403
{(D1, D2, D4), D3}	8533	22	13	0	1838	6928	19	11	3	1471	1605	3	2	367
{(D1, D2, D3, D4)}	8706	22	13	0	2145	7051	19	11	3	1741	1655	3	2	404
{D1, D2, D3, D4}	8029	16	12	0	2020	6476	13	10	5	1348	1953	3	2	672

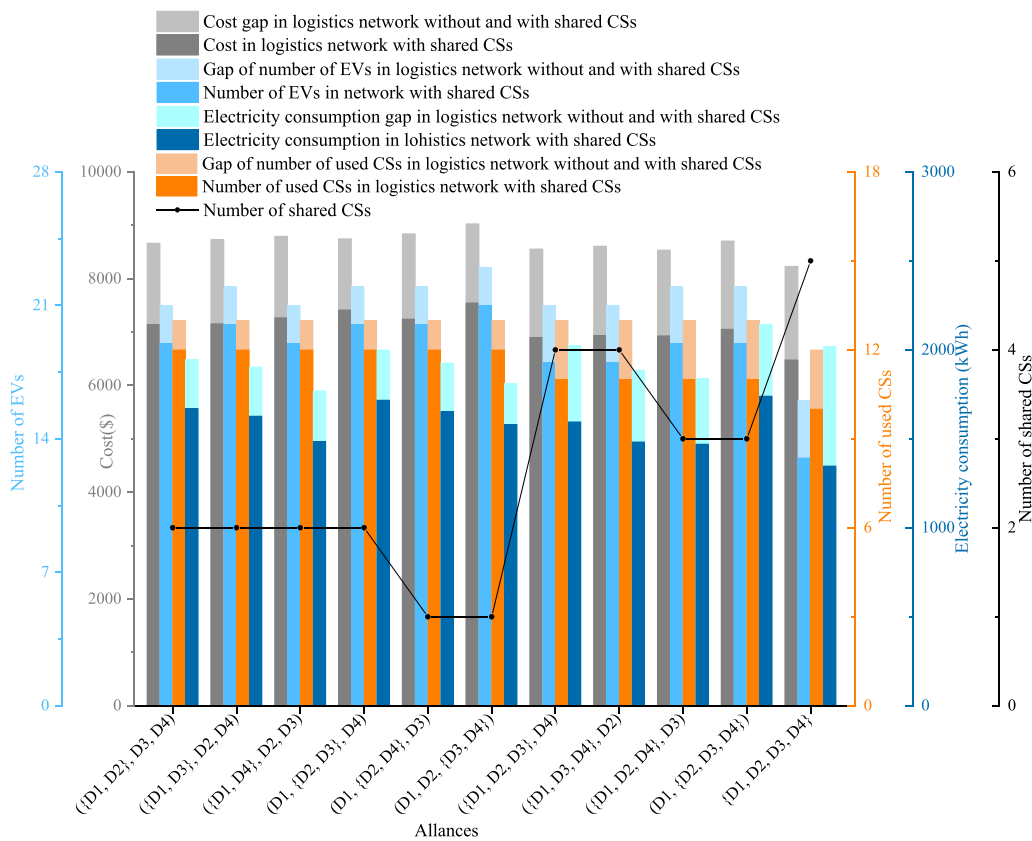


Fig. 19. Comparison results of various alliances.

When a collaborative alliance is established, customers can be reassigned to appropriate depots by customer service sharing to avoid long-distance transportation and violations of time windows. The delivery routes and charging determinations are coordinated by solving the CMEVRPTW-SCS to achieve electricity consumption savings. The implementation of the CS sharing strategy among various depots can reduce the number of used CSs to improve resource utilization, and increase the number of EV service customers on a route to reduce the

number of required EVs. Therefore, the collaborative mechanism and the CS sharing strategy can realize the resource and cost savings of the whole transportation system and produce positive environmental effects.

(2) An appropriate solution methodology is critical to solve the CMEVRPTW-SCS effectively. On the one hand, a bi-objective nonlinear programming model formulated for minimizing the operating cost and number of EVs under the time window and energy constraints can offer a

Table 25
Route comparison of D1 and D4 in the optimized network without and with shared CSs.

Scenarios	Depots	Routes	Total Cost (\$)	Cost (\$)	Number of EVs	EC (kWh)	Total EC (kWh)
Optimized network without shared CSs	D1	C4 → C3 → C6 → C8 → C20 → C23 → CS3 → C35 → C36 → C16 → C7 C17 → C22 → C33 → C29 → CS4 → C31 → C21 → C9 C13 → C18 → C34 → C26 → C27 → CS11 → C54 → C11 C10 → C5 → C2 → C1 → C15 → C24 → CS1 → C14 → C19 → C12	4056	1883	4	439	912
	D4	C107 → C125 → C127 → C123 → C135 C138 → C141 → CS2 → C143 → C142 → C139 → C43 C129 → C134 → C133 → C132 → C131 → C130 → CS10 → C128 → 121 → 122 → 126 → 124 C30 → C137 → C136 → C28 → C140	2173		4		473
Optimized network with shared CSs	D1	C10 → C5 → C2 → C1 → C15 → C24 → CS1 → C13 → C18 → C34 → C14 → C11 C4 → C3 → C6 → C8 → C20 → C23 → CS3* → C31 → C21 → C9 C12 → C19 → C25 → C26 → C27 → CS11* → C54 → C17 → C22 → C33 → CS2* → C29 → C36 → C16 → C35 → C7	3093	1491	3	317	649
	D4	C107 → C125 → C127 → C122 → C126 → C124 C135 → C134 → C136 → CS11* → C133 → C132 → C131 → C130 → CS10 → C128 → C121 → C123 → C129 C30 → C138 → C137 → C28 → C140 → C141 → CS2* → C143 → C142 → C139 → C43	1602		3		332

CS: used charging stations.

CS*: shared charging stations.

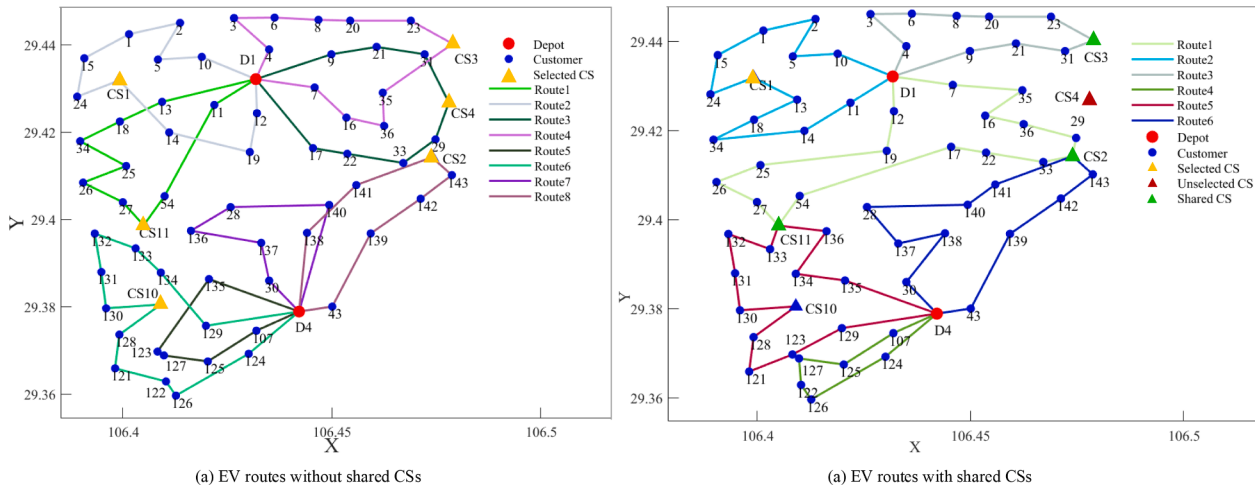


Fig. 20. EV routes of D1 and D4 without and with shared CSs.

reference for EVs' routing optimization. On the other hand, effective vehicle scheduling schemes derived from a hybrid heuristic algorithm combining GMCA with IMOGA-TS can achieve the coordination of customer service among multiple depots, and determine the optimal routes with the maximum cost reduction and the minimum electricity consumption. In addition, the experimental calculation results indicate the effectiveness and adaptability of the proposed mathematical model and hybrid algorithm in improving the large-scale EVs' distribution network and obtaining the optimal EV routes.

(3) The implementation of carbon peak and carbon neutrality has provided great opportunities for the popularization and development of new energy vehicles. The government has issued a series of policies to optimize the basic charging facility configuration, and promote the collaborative development of vehicle stations, thus providing a broad space for the development and popularization of EV distribution. In addition, the new energy technologies (e.g., vehicle pile cloud interconnection, wireless charging, new battery technologies, and orderly charging management technology) are promising in promoting the collaborative interaction of energy and information between EVs and smart grids, thus systematically solving the difficulty in EVs' en-route charging. Therefore, the long-term collaboration among multiple logistics facilities and CS sharing strategy should be widely adopted as an effective way to build a fully functional, reasonably laid out, stably operational, intelligent and safe EV distribution network.

7. Conclusions

In this study, the collaborative mechanism and the CS sharing strategy are introduced to integrate resources and optimize EVs' delivery routes. To improve the operation efficiency of the EV distribution network and realize reasonable resource configuration, the following three aspects are mainly implemented. First, a bi-objective nonlinear optimization model is constructed to minimize the operating cost and the number of EVs. Second, a hybrid heuristic algorithm combining GMCA with the IMOGA-TS algorithm is proposed to achieve the optimal solution of the CMEVRPTW-SCS. Finally, a cooperative alliance strategy based on the Shapley value model is proposed to obtain the optimal profit allocation strategy in the EV distribution network.

We compare the proposed IMOGA-TS with MOGA, NSGA-II and MOHSA, and the comparison results have shown the superiority of the proposed IMOGA-TS in solving CMEVRPTW-SCS optimization and providing high-quality Pareto optimal solution. Then, an empirical study is implemented to evaluate the practical significance of the proposed model and algorithm in a real CMEVRPTW-SCS optimization case in Chongqing City, China. Compared with the initial logistics network,

the total operating cost is reduced from \$12,047 to \$6,476, with a reduction rate of 46.2 %. In addition, the number of EVs decreases from 29 to 13, with a drop of 16, and the electricity consumption of EVs decreases from 4,144 to 1,348 kWh, with a decrement of 67 %. The experimental calculation results demonstrate that the proposed methodology in this study is effective in reducing operating costs, the number of EVs, and electricity consumption in the CMEVRPTW-SCS. In addition, Shapley value model is selected to allocate profit, which helps in using profit allocation as a mechanism to motivate multiple depots to collaborate.

The sensitivity analysis of collaboration schemes indicates that the collaborative mechanism and the CS sharing strategy play an important role. Three scenarios of collaboration schemes are analyzed and discussed, and the comparison results prove the effectiveness of the collaborative mechanism in the optimization of logistics networks. Moreover, CS sharing situations in 11 various alliances are explored and compared, and the comparison result justifies the superiority of collaboration and the CS sharing strategy in the CMEVRPTW-SCS optimization. Therefore, the collaborative mechanism and the CS sharing strategy should be encouraged to construct sustainable and economic logistics networks for logistics enterprises and managers.

Future research can be carried out in the following directions: (1) The simultaneous pickup and delivery service can be integrated into the MDEVRPTW. (2) Dynamic customer demands can be incorporated in an EV distribution network optimization. (3) The sharing of EVs can be explored in the logistics network optimization to facilitate collaboration, and a sustainable collaborative system can be constructed. (4) The problem that each CS can be used multiple times by all routes in an EV distribution network should be investigated, and the corresponding algorithm solution presentation should be further studied. (5) The combination of battery swap and charging can be further studied in the collaboration framework to alleviate the range anxiety with EVs.

CRediT authorship contribution statement

Yong Wang: Conceptualization, Methodology, Funding acquisition, Data curation, Formal analysis, Investigation, Project administration, Software, Validation, Supervision, Resources, Visualization, Writing – original draft, Writing – review & editing. **Jingxin Zhou:** Conceptualization, Methodology, Data curation, Formal analysis, Investigation, Software, Validation, Writing – original draft, Writing – review & editing. **Yaoyao Sun:** Conceptualization, Methodology, Software, Validation, Writing – original draft, Writing – review & editing. **Jianxin Fan:** Funding acquisition, Project administration, Supervision, Resources, Visualization, Writing – original draft, Writing – review & editing.

Zheng Wang: Funding acquisition, Project administration, Supervision, Resources, Visualization. **Haizhong Wang:** Supervision, Resources, Visualization.

Declaration of Competing Interest

The authors declare that they have no known competing financial interests or personal relationships that could have appeared to influence the work reported in this paper.

Data availability

Data will be made available on request.

Acknowledgments

The authors would like to express our sincere appreciation for the valuable comments made by two anonymous reviewers, which helped us to improve the quality of this paper. This research is supported by National Natural Science Foundation of China (Project No. 71871035, 71971036, 41977337), Natural Science Foundation of Chongqing, China (CSTB2022NSCQ-MSX0535), Key Science and Technology Research Project of Chongqing Municipal Education Commission (KJZD-K202000702), Chongqing Liuchuang Plan Innovation Project (cx2021038), Team Building Project for Graduate Tutors in Chongqing (JDDSTD2019008), Chongqing Bayu Scholar Youth Project (YS2021058).

References

- Almouhanna, A., Quintero-Araujo, C. L., Panadero, J., Juan, A. A., Khosravi, B., & Ouelhadj, D. (2020). The location routing problem using electric vehicles with constrained distance. *Computers & Operations Research*, 115, Article 104864.
- Aloui, A., Hamani, N., & Delahocie, L. (2021). An integrated optimization approach using a collaborative strategy for sustainable cities freight transportation: A Case study. *Sustainable Cities and Society*, 75, Article 103331.
- Asghari, M., & Al-e-hashem, S. M. J. M. (2021). Green vehicle routing problem: A state-of-the-art review. *International Journal of Production Economics*, 231, Article 107899.
- Bac, U., & Erdem, M. (2021). Optimization of electric vehicle recharge schedule and routing problem with time windows and partial recharge: A comparative study for an urban logistics fleet. *Sustainable Cities and Society*, 70, Article 102883.
- Bae, H., & Moon, I. (2016). Multi-depot vehicle routing problem with time windows considering delivery and installation vehicles. *Applied Mathematical Modelling*, 40 (13–14), 6536–6549.
- Basso, R., Kulcsár, B., & Sanchez-Díaz, I. (2021). Electric vehicle routing problem with machine learning for energy prediction. *Transportation Research Part B: Methodological*, 145, 24–55.
- Cai, L., Wang, X., Luo, Z. X., & Liang, Y. J. (2022). A hybrid adaptive large neighborhood search and tabu search algorithm for the electric vehicle relocation problem. *Computers & Industrial Engineering*, 167, Article 108005.
- China Central Television Finance.com (CCTV.com). (2021). Recurrence of range anxiety. Retrieved from <<https://tv.cctv.com/2021/12/25/VIDEZmAQ3MhkTVTnfpdaczF211225.shtml>> on January 11, 2022.
- Chen, S. F., Chen, R., & Gao, J. (2017). A Modified harmony search algorithm for solving the dynamic vehicle routing problem with time windows. *Scientific Programming*, 2017, 1021432.
- Chen, Y. R., Li, D. C., Zhang, Z. C., Wahab, M. I. M., & Jiang, Y. S. (2021). Solving the battery swap station location-routing problem with a mixed fleet of electric and conventional vehicles using a heuristic branch-and-price algorithm with an adaptive selection scheme. *Expert Systems with Applications*, 186, Article 115683.
- China Electric Vehicle Charging Infrastructure Promotion Alliance (CEVCIPA). (2021). Statistical summary of charging facilities in Charging Alliance: 2019–12. Retrieved from <<http://www.evcpa.org.cn/>> on January 11, 2022.
- Cleophas, C., Cottrill, C., Ehmke, J. F., & Tierney, K. (2019). Collaborative urban transportation: Recent advances in theory and practice. *European Journal of Operational Research*, 273(3), 801–816.
- Comi, A., Schiraldi, M. M., & Buttarazzi, B. (2018). Smart urban freight transport: Tools for planning and optimising delivery operations. *Simulation Modelling Practice and Theory*, 88, 48–61.
- Cortés-Murcia, D. L., Prodhon, C., & Afsar, H. M. (2019). The electric vehicle routing problem with time windows, partial recharges and satellite customers. *Transportation Research Part E: Logistics and Transportation Review*, 130, 184–206.
- Desaulniers, G., Errico, F., Irnich, S., & Schneider, M. (2016). Exact algorithms for electric vehicle-routing problems with time windows. *Operations Research*, 64(6), 1388–1405.
- Erdelic, T., Caric, T., Erdelic, M., & Tisljaric, L. (2019). Electric vehicle routing problem with single or multiple recharges. *Transportation Procedia*, 40, 217–224.
- Erdem, M., & Koç, Ç. (2019). Analysis of electric vehicles in home health care routing problem. *Journal of Cleaner Production*, 234, 1471–1483.
- Feng, F., Pang, Y. S., Lodewijks, G., & Li, W. F. (2017). Collaborative framework of an intelligent agent system for efficient logistics transport planning. *Computers & Industrial Engineering*, 112, 551–567.
- Ghannadpour, S. F., & Zandiye, F. (2020). An adapted multi-objective genetic algorithm for solving the cash in transit vehicle routing problem with vulnerability estimation for risk quantification. *Engineering Applications of Artificial Intelligence*, 96, Article 103964.
- Ghobadi, A., Tavakkoli-Moghaddam, R., Fallah, M., & Kazemipoor, H. (2021). Multi-depot electric vehicle routing problem with fuzzy time windows and pickup/delivery constraints. *Journal of Applied Research on Industrial Engineering*, 8, 1–18.
- Gmira, M., Gendreau, M., Lodi, A., & Potvin, J. Y. (2021). Tabu search for the time-dependent vehicle routing problem with time windows on a road network. *European Journal of Operational Research*, 288(1), 129–140.
- Goeke, D. (2019). Granular tabu search for the pickup and delivery problem with time windows and electric vehicles. *European Journal of Operational Research*, 278(3), 821–836.
- Goeke, D., & Schneider, M. (2015). Routing a mixed fleet of electric and conventional vehicles. *European Journal of Operational Research*, 245(1), 81–99.
- Granada-Echeverri, M., Cubides, L. C., & Bustamante, J. O. (2020). The electric vehicle routing problem with backhauls. *International Journal of Industrial Engineering Computations*, 11(1), 131–152.
- Hiermann, G., Hartl, R. F., Puchinger, J., & Vidal, T. (2019). Routing a mix of conventional, plug-in hybrid, and electric vehicles. *European Journal of Operational Research*, 272(1), 235–248.
- Hiermann, G., Puchinger, J., Ropke, S., & Hartl, R. F. (2016). The electric fleet size and mix vehicle routing problem with time windows and recharging stations. *European Journal of Operational Research*, 252(3), 995–1018.
- Jia, W. Z., Tan, Y. Y., Liu, L., Li, J., Zhang, H. X., & Zhao, K. (2019). Hierarchical prediction based on two-level Gaussian mixture model clustering for bike-sharing system. *Knowledge-Based Systems*, 178, 84–97.
- Jouida, S. B., Guajardo, M., Klifi, W., & Krichen, S. (2021). Profit maximizing coalitions with shared capacities in distribution networks. *European Journal of Operational Research*, 288(2), 480–495.
- Kancharla, S. R., & Ramadurai, G. (2020). Electric vehicle routing problem with non-linear charging and load-dependent discharging. *Expert Systems with Applications*, 160, Article 113714.
- Karakatić, S. (2021). Optimizing nonlinear charging times of electric vehicle routing with genetic algorithm. *Expert Systems with Applications*, 164, Article 114039.
- Karakatić, S., & Podgorelec, V. (2015). A survey of genetic algorithms for solving multi-depot vehicle routing problem. *Applied Soft Computing*, 27, 519–532.
- Katoch, S., Chauhan, S. S., & Kumar, V. (2021). A review on genetic algorithm: Past, present, and future. *Multimedia Tools and Applications*, 80(5), 8091–8126.
- Keskin, M., & Çatay, B. (2016). Partial recharge strategies for the electric vehicle routing problem with time windows. *Transportation Research Part C: Emerging Technologies*, 65, 111–127.
- Keskin, M., & Çatay, B. (2018). A matheuristic method for the electric vehicle routing problem with time windows and fast chargers. *Computers & Operations Research*, 100, 172–188.
- Keskin, M., Çatay, B., & Laporte, G. (2021). A simulation-based heuristic for the electric vehicle routing problem with time windows and stochastic waiting times at recharging stations. *Computers & Operations Research*, 125, Article 105060.
- Keskin, M., Laporte, G., & Çatay, B. (2019). Electric vehicle routing problem with time-dependent waiting times at recharging stations. *Computers & Operations Research*, 107, 77–94.
- Koç, Ç., Jabali, O., Mendoza, J. E., & Laporte, G. (2019). The electric vehicle routing problem with shared charging stations. *International Transactions in Operational Research*, 26(4), 1211–1243.
- Konstantakopoulos, G. D., Gayialis, S. P., & Kechagias, E. P. (2020). Vehicle routing problem and related algorithms for logistics distribution: A literature review and classification. *Operational Research*. <https://doi.org/10.1007/s12351-020-00600-7>
- Kucukoglu, I., Dewil, R., & Catrysse, D. (2021). The electric vehicle routing problem and its variations: A literature review. *Computers & Industrial Engineering*, 161, Article 107650.
- Küçükoglu, I., Dewil, R., & Dirk, C. (2019). Hybrid simulated annealing and tabu search method for the electric travelling salesman problem with time windows and mixed charging rates. *Expert Systems with Applications*, 134, 279–303.
- Li, Y., Lim, M. K., Tan, Y. S., Lee, S. Y., & Tseng, M. L. (2020). Sharing economy to improve routing for urban logistics distribution using electric vehicles. *Resources, Conservation and Recycling*, 153, Article 104585.
- Li, Y., Lim, M. K., & Wang, C. (2022). An intelligent model of green urban distribution in the blockchain environment. *Resources, Conservation and Recycling*, 176, Article 105925.
- Li, Y. B., Soleimani, H., & Zohal, M. (2019). An improved ant colony optimization algorithm for the multi-depot green vehicle routing problem with multiple objectives. *Journal of Cleaner Production*, 227, 1161–1172.
- Lin, J., Zhou, W., & Wolfson, O. (2016). Electric vehicle routing problem. *Transportation Research Procedia*, 12, 508–521.
- Long, J. Y., Sun, Z. Z., Pardalos, P. M., Hong, Y., Zhang, S. H., & Li, C. (2019). A hybrid multi-objective genetic local search algorithm for the prize-collecting vehicle routing problem. *Information Sciences*, 478, 40–61.
- Lu, J., Chen, Y. N., Hao, J. K., & He, R. J. (2020). The Time-dependent Electric Vehicle Routing Problem: Model and solution. *Expert Systems with Applications*, 161, Article 113593.

- Mai, F., Fry, M. J., & Ohlmann, J. W. (2018). Model-based capacitated clustering with posterior regularization. *European Journal of Operational Research*, 271(2), 594–605.
- Mancini, S., Gansterer, M., & Hartl, R. F. (2021). The collaborative consistent vehicle routing problem with workload balance. *European Journal of Operational Research*, 293(3), 955–965.
- Melo, S. A., Pereira, R. B. D., Reis, A. F. S., Lauro, C. H., & Brandão, L. C. (2022). Multi-objective evolutionary optimization of unsupervised latent variables of turning process. *Applied Soft Computing*, 120, Article 108713.
- Mesa-Arango, R., & Ukkusuri, S. V. (2015). Demand clustering in freight logistics networks. *Transportation Research Part E: Logistics and Transportation Review*, 81, 36–51.
- Moghdani, R., Salimifard, K., Demir, E., & Benyettou, A. (2021). The green vehicle routing problem: A systematic literature review. *Journal of Cleaner Production*, 279, Article 123691.
- Mohammed, M. A., Abd Ghani, M. K., Hamed, R. I., Mostafa, S. A., Ahmad, M. S., & Ibrahim, D. A. (2017). Solving vehicle routing problem by using improved genetic algorithm for optimal solution. *Journal of Computational Science*, 21, 255–262.
- Montoya, A., Guéret, C., Mendoza, J. E., & Villegas, J. G. (2017). The electric vehicle routing problem with nonlinear charging function. *Transportation Research Part B: Methodological*, 103, 87–110.
- Muñoz-Villamizar, A., Montoya-Torres, J. R., & Faulin, J. (2017). Impact of the use of electric vehicles in collaborative urban transport networks: A case study. *Transportation Research Part D: Transport and Environment*, 50, 40–54.
- Nolz, P. C., Absi, N., Feillet, D., & Seragiotti, C. (2022). The consistent electric-Vehicle routing problem with backhauls and charging management. *European Journal of Operational Research*. <https://doi.org/10.1016/j.ejor.2022.01.024>
- Owais, M., & Osman, M. K. (2018). Complete hierarchical multi-objective genetic algorithm for transit network design problem. *Expert Systems with Applications*, 114, 143–154.
- Pardo-Bosch, F., Pujadas, P., Morton, C., & Cervera, C. (2021). Sustainable deployment of an electric vehicle public charging infrastructure network from a city business model perspective. *Sustainable Cities and Society*, 71, Article 102957.
- Park, H., Son, D., Koo, B., & Jeong, B. (2021). Waiting strategy for the vehicle routing problem with simultaneous pickup and delivery using genetic algorithm. *Expert Systems with Applications*, 165, Article 113959.
- Pierre, D. M., & Zakaria, N. (2017). Stochastic partially optimized cyclic shift crossover for multi-objective genetic algorithms for the vehicle routing problem with time-windows. *Applied Soft Computing*, 52, 863–876.
- Qiu, M., Fu, Z., Eglese, R., & Tang, Q. (2018). A tabu search algorithm for the vehicle routing problem with discrete split deliveries and pickups. *Computers & Operations Research*, 100, 102–116.
- Rabbani, M., Farrokhi-Asl, H., & Asgarian, B. (2016). Solving a bi-objective location routing problem by a NSGA-II combined with clustering approach: Application in waste collection problem. *Journal of Industrial Engineering International*, 13(1), 13–27.
- Raeesi, R., & Zografos, K. G. (2022). Coordinated routing of electric commercial vehicles with intra-route recharging and en-route battery swapping. *European Journal of Operational Research*, 301(1), 82–109.
- Rezgui, D., Chaouachi Siala, J., Aggoun-Mtalaa, W., & Bouziri, H. (2019). Application of a variable neighborhood search algorithm to a fleet size and mix vehicle routing problem with electric modular vehicles. *Computers & Industrial Engineering*, 130, 537–550.
- Robert, R., & Wen, M. (2016). The electric traveling salesman problem with time windows. *Transportation Research Part E: Logistics and Transportation Review*, 89, 32–52.
- Sadati, M. E. H., Çatay, B., & Aksen, . (2021). An efficient variable neighborhood search with tabu shaking for a class of multi-depot vehicle routing problems. *Computers & Operations Research*, 133, Article 105269.
- Santos, M. J., Martins, S., Amorim, P., & Almada-Lobo, B. (2021). A green lateral collaborative problem under different transportation strategies and profit allocation methods. *Journal of Cleaner Production*, 288, Article 125678.
- Schiffer, M., & Walther, G. (2017). The electric location routing problem with time windows and partial recharging. *European Journal of Operational Research*, 260(3), 995–1013.
- Schneider, M., Stenger, A., & Goeke, D. (2014). The electric vehicle routing problem with time windows and recharging stations. *Transportation Science*, 48(4), 500–520.
- Sethanan, K., & Jamrus, T. (2020). Hybrid differential evolution algorithm and genetic operator for multi-trip vehicle routing problem with backhauls and heterogeneous fleet in the beverage logistics industry. *Computers & Industrial Engineering*, 146, Article 106571.
- Shao, S., Guan, W., & Bi, J. (2018). Electric vehicle routing problem with charging demands and energy consumption. *IET Intelligent Transport Systems*, 12(3), 202–212.
- Soto, M., Sevaux, M., Rossi, A., & Reinholz, A. (2017). Multiple neighborhood search, tabu search and ejection chains for the multi-depot open vehicle routing problem. *Computers & Industrial Engineering*, 107, 211–222.
- Vaziri, S., Etebari, F., & Vahdani, B. (2019). Development and optimization of a horizontal carrier collaboration vehicle routing model with multi-commodity request allocation. *Journal of Cleaner Production*, 224, 492–505.
- Verma, A. (2018). Electric vehicle routing problem with time windows, recharging stations and battery swapping stations. *Euro Journal on Transportation and Logistics*, 7(4), 415–451.
- Wang, Y., Li, Q., Guan, X. Y., Fan, J. X., Xu, M. Z., & Wang, H. Z. (2021). Collaborative multi-depot pickup and delivery vehicle routing problem with split loads and time windows. *Knowledge-Based Systems*, 231, Article 107421.
- Wang, Y., Li, Q., Guan, X. Y., Xu, M. Z., Liu, Y., & Wang, H. Z. (2021). Two-echelon collaborative multi-depot multi-period vehicle routing problem. *Expert Systems with Applications*, 167, Article 114201.
- Wang, Y., Ma, X. L., Li, Z. B., Liu, Y., Xu, M. Z., & Wang, Y. H. (2017). Profit distribution in collaborative multiple centers vehicle routing problem. *Journal of Cleaner Production*, 144, 203–219.
- Wang, Y., Peng, S. G., & Xu, M. (2021). Emergency logistics network design based on space-time resource configuration. *Knowledge-Based Systems*, 223, Article 107041.
- Wang, Y., Peng, S. G., Zhou, X. S., Mahmoudi, M., & Zhen, L. (2020). Green logistics location-routing problem with eco-packages. *Transportation Research Part E: Logistics and Transportation Review*, 143, Article 102118.
- Wang, Y., Wang, Z., Hu, X. P., Xue, G. Q., & Guan, X. Y. (2022). Truck-drone hybrid routing problem with time-dependent road travel time. *Transportation Research Part C: Emerging Technologies*, 144, Article 103901.
- Wang, J. W., Yu, Y., & Tang, J. F. (2018). Compensation and profit distribution for cooperative green pickup and delivery problem. *Transportation Research Part B: Methodological*, 113, 54–69.
- Wang, Y., Yuan, Y. Y., Guan, X. Y., Xu, M. Z., Wang, L., Wang, H. Z., & Liu, Y. (2020). Collaborative two-echelon multicenter vehicle routing optimization based on state-space-time network representation. *Journal of Cleaner Production*, 258, Article 120590.
- Wang, Y., Zhang, J., Guan, X. Y., Xu, M. Z., Wang, Z., & Wang, H. Z. (2021). Collaborative multiple centers fresh logistics distribution network optimization with resource sharing and temperature control constraints. *Expert Systems with Applications*, 165, Article 113838.
- Wang, Y., Zhe, J. Y., Wang, X. W., Fan, J. X., Wang, Z., & Wang, H. Z. (2022). Collaborative multicenter reverse logistics network design with dynamic customer demands. *Expert Systems with Applications*, 206, Article 117926.
- Wei, X. W., Qiu, H. X., Wang, D., Duan, J. H., Wang, Y. Z., & Cheng, T. C. E. (2020). An integrated location-routing problem with post-disaster relief distribution. *Computers & Industrial Engineering*, 147, Article 106632.
- Wen, M., Linde, E., Ropke, S., Mirchandani, P., & Larsen, A. (2016). An adaptive large neighborhood search heuristic for the electric vehicle scheduling problem. *Computers & Operations Research*, 76, 73–83.
- Wu, W. T., Lin, Y., Liu, R. H., & Jin, W. Z. (2022). The multi-depot electric vehicle scheduling problem with power grid characteristics. *Transportation Research Part B: Methodological*, 155, 322–347.
- Xu, Z. T., Elomri, A., Pokharel, S., & Mutlu, F. (2019). A model for capacitated green vehicle routing problem with the time-varying vehicle speed and soft time windows. *Computers & Industrial Engineering*, 137, Article 106011.
- Yang, S. Y., Ning, L. J., Tong, L. C., & Shang, P. (2021). Optimizing electric vehicle routing problems with mixed backhauls and recharging strategies in multi-dimensional representation network. *Expert Systems with Applications*, 176, Article 114804.
- Yang, J., & Sun, H. (2015). Battery swap station location-routing problem with capacitated electric vehicles. *Computers & Operations Research*, 55, 217–232.
- Yassen, E. T., Ayob, M., Nazri, M. Z. A., & Sabar, N. R. (2017). An adaptive hybrid algorithm for vehicle routing problems with time windows. *Computers & Industrial Engineering*, 113, 382–391.
- Zang, Y. S., Wang, M. Q., & Qi, M. Y. (2022). A column generation tailored to electric vehicle routing problem with nonlinear battery depreciation. *Computers & Operations Research*, 137, Article 105527.
- Zarouk, Y., Mahdavi, I., Rezaeian, J., & Santos-Arteaga, F. J. (2022). A novel multi-objective green vehicle routing and scheduling model with stochastic demand, supply, and variable travel times. *Computers & Operations Research*, 141, Article 105698.
- Zhang, S., Chen, M. Z., & Zhang, W. Y. (2019). A novel location-routing problem in electric vehicle transportation with stochastic demands. *Journal of Cleaner Production*, 221, 567–581.
- Zhang, S., Gajpal, Y., Appadoo, S. S., & Abdulkader, M. M. S. (2018). Electric vehicle routing problem with recharging stations for minimizing energy consumption. *International Journal of Production Economics*, 203, 404–413.
- Zon, M., & Desaulniers, G. (2021). The joint network vehicle routing game with optional customers. *Computers & Operations Research*, 133, Article 105375.